Influence of covariance of aerosol and meteorology on co-located precipitating and non-precipitating clouds over Indo-Gangetic Plains

Nabia Gulistan[1], Khan Alam[1*], Yangang Liu[2]

[1]Department of Physics, University of Peshawar, Peshawar, 25120, Pakistan
[2]Environmental & Climate Science Department, Brookhaven National Laboratory, USA

*Correspondence: Khan Alam (khanalam@uop.edu.pk)

HIGHLIGHTS

- Strong aerosol-cloud relations under unstable meteorological conditions led to the formation of thick precipitating clouds.
- In thick clouds, the activation of cloud droplets is weakly dependent on aerosols.
- Optically thin clouds led to a high precipitation rate.

ABSTRACT

Aerosol-cloud-precipitation-interaction (ACPI) plays a pivotal role in the global and regional water cycle and the earth's energy budget; however, it remains highly uncertain due to the underlying different physical mechanisms. Therefore, this study aims to systematically analyze the effects of aerosols and meteorological factors on ACPI in the co-located precipitating (PCs) and non-precipitating clouds (NPCs) clouds in winter and summer seasons by employing the long-term (2001-2021) retrievals from Moderate Resolution Imaging Spectroradiometer (MODIS), Tropical Rainfall Measuring Mission (TRMM) coupled with the National Center for Environmental Prediction/National Center for Atmospheric Research (NCEP/NCAR) reanalysis-II datasets over the Indo-Gangetic Plains (IGP). The results exhibit a decadal increase in aerosol optical depth (AOD) over Lahore (5.2%), Delhi (9%), Kanpur (10.7%), and Gandhi College (22.7%) and a decrease over Karachi (-1.9%) and Jaipur (-0.5%). The most stable meteorology with high values of lower tropospheric stability (LTS) is found in both seasons over Karachi. In the summer season, the occurrence frequency of clouds is high (74%) over Gandhi College, 60% of which are PCs. Conversely, the least number of PCs are found over Karachi. Similarly, in the winter season, the frequency of cloud occurrence is low over Karachi and high over Lahore and Gandhi College. The analysis of cloud top pressure (CTP) and cloud optical thickness (COT) indicate high values of cloud fraction (CF) for thick and high-level clouds over all study areas except Karachi. The microphysical properties such as cloud effective radius (CER) and cloud droplet number

concentration (CDNC) bear high values (CER $> \sim 15$ μm and CDNC $> \sim 50$ cm^{-3}) for both NPCs and PCs in summer. The AOD-CER correlation is good (weak) for PCs (NPCs) in winter. Similarly, the sensitivity value of the first indirect effect (FIE) is high (ranging from 0.2 ± 0.13 to 0.3 ± 0.01 in winter, and from 0.19 ± 0.03 to 0.32 ± 0.05 in summer) for PCs and low for NPCs. The sensitivity value for the second indirect effect (SIE) is relatively higher (such as 0.6 ± 0.14 in winter and 0.4 ± 0.04 in summer) than FIE. Sensitivity values of the aerosol-cloud interaction (ACI) are low (i.e., -0.06 ± 0.09) for PCs in summer. Furthermore, the precipitation rate (PR) exhibits high values in summer season, primarily due to the significant contribution from optically thick clouds with lower CDNC ($< \sim 50$ cm^{-3}) and larger CER, and intermediate contribution from optically thick clouds with higher CDNC ($> \sim 50$ cm^{-3}).

Keywords: Aerosol-cloud-precipitation-interaction, Aerosol optical depth, cloud effective radius, cloud droplet number concentration, lower tropospheric stability, relative humidity, first indirect effect, second indirect effect, precipitation sensitivity.

1. Introduction

The aerosol-cloud-precipitation-interaction (ACPI) and aerosol-radiation-interaction (ARI) significantly influence climates at the regional and global scales (Romero et al., 2021). Assessing the direct and indirect effects of aerosols is crucial to understanding and predicting the energy budget and the water cycle. In the direct effect, the absorption and scattering of solar radiation by aerosols lead to the warming of the atmosphere and cooling of the earth's surface (Zhou et al., 2020), causing changes in the lower tropospheric stability (LTS) that further lead to modulation of precipitating (PCs) and non-precipitation clouds (NPCs) (Andreae & Rosenfeld, 2008). Precipitating clouds are thick clouds with significant vertical development and high moisture content form under unstable atmospheric conditions, such as cumulonimbus and nimbostratus, that produce precipitation reaching the ground. In contrast, non-precipitating clouds are typically thin, have low moisture content, and form under stable atmospheric conditions, including cloud types like cirrus, cirrostratus, altostratus, and stratus, which generally do not produce significant precipitation (Houze Jr, 2014).

60 In the indirect effect, the water-soluble aerosols such as soil dust, sulfates, nitrates, and other

61 organic aerosols ejected naturally and anthropogenically serve as cloud condensation nuclei (CCN)

62 and ice nucleating particles (INP). Hence, aerosols affect the aerosol-cloud-interaction (ACI) by

63 influencing the growth of cloud droplets and cloud droplet number concentration (CDNC)

64 (Twomey et al., 1977; Albrecht, 1989; Jiang et al., 2002; Chen et al., 2011; Tao et al., 2012). The

65 increase of CDNC and decrease of cloud droplet effective radius (CER) inhibit the onset of

66 precipitation and increase the cloud lifetime (Albrecht, 1989). Conversely, the decrease in CDNC

67 and increase in CER increases the probability of precipitation rate (PR). Conversely, Stevens and

68 Feingold (2009) have shown that initially, more sea salt carried by high wind speed inhibits

69 precipitation formation. However, the same sea spray tends to seed the coalescence by producing

70 larger CER that leads to enhanced precipitation.

71 In the last few decades, most of the cultivable land of the Indo-Gangetic Plain (IGP) has been

72 replaced by urban developments. Due to the fastest growth of population, urbanization,

73 industrialization, and massive combustion of biomass and fossil fuels in residential homes and

74 factories, a decadal increase in aerosols is observed over IGP. The high aerosol loading may affect

75 the formation of tropospheric clouds and seasonal precipitation patterns (Kaskaoutis et al., 2011;

76 Singh et al., 2015; Thomas et al., 2021). The high aerosol loading makes IGP suitable for the study

77 of ACPI. Besides, frequent variations in cloud fraction (CF), extreme precipitation and drought

78 abrupt temperature changes (e.g., heat waves), and irregular unseasonal rains may cause major and

79 unavoidable hazards at local and regional levels in the future (Zhou et al., 2020).

80 In the last two decades, the scientific community has focused on quantification of ACI using both

81 observations (Feingold et al., 2003; Koren et al., 2004; Costantino et al., 2010; Wang et al., 2015;

82 Zhao et al., 2018, Guo et al., 2019; 2020; Anwar et al., 2022) and modeling techniques (Chen et

83 al., 2016, 2018; Wang et al. 2020; Zhou et al., 2020; Sharma et al., 2023). Although, a similar

84 recent study (Anwar et al., 2022) attempted to understand the sensitivities of ACI and the first

85 indirect effect of different subsets of AOD to the different conditions of RH and wind directions

86 and found a decrease (increase) in CER with aerosol loading Twomey effect (anti-Twomey effect)

87 over the monsoon (weak and moderately intensive monsoon) regions. However, the above study

88 excluded the other significant meteorological parameters such as LTS, PR, and T_{850} and was also

89 limited to the monsoon regions of Pakistan only. Further, in the context of warm rain processes, it

90   is generally understood that the high concentration of aerosols capable of serving as CCN leads to

91   enhanced CDNC known as the first indirect effect (FIE) or Twomey effect (Twomey et al., 1977).

92   It is also widely acknowledged that CDNC plays a pivotal role in cloud microphysics and

93   significantly influences the onset of precipitation and retention of water in clouds called the second

94   indirect effect (SIE) (Gryspeerdt et al., 2016; Naud et al., 2017). Whilst, in the above study, the

95   analysis of CDNC is also not addressed. Therefore, the present study aims to deepen the previous

96   study (Anwar et al., 2022), by a long-term and detailed analysis of the ACPI including aerosol-

97   indirect effects for low-level liquid clouds extended over the whole IGP for understanding different

98   mechanisms (condensation, droplet growth and precipitation rate) of cloud and precipitation

99   formation.

100   This study is focused on estimating the variations in sensitivities of aerosol-cloud relationship to

101   the variations in aerosol loading at specified meteorological conditions for low-level PCs and

102   NPCs in the summer and winter seasons over the IGP. This study is unique in using a large number

103   of samples, classification of liquid clouds in PCs and NPCs, further classification of clouds in low,

104   mid, and high-level clouds through joint COT-CTP histograms, quantification of the sensitivities

105   of FIE, SIE, total indirect effect (TIE), and ACI to CDNC. The significant meteorological

106   parameters considered include temperature at 850 hPa, LTS, relative humidity (RH%) at 850 hPa,

107   vertical velocity (ω), and PR. Furthermore, by utilizing the Moderate Resolution Imaging

108   Spectroradiometer (MODIS) and Tropical Rainfall Measuring Mission (TRMM) data, the

109   correlation of cloud microphysical properties (CER and CDNC) and AOD at specified values of

110   LTS and cloud liquid water path (CLWP) is examined, and precipitation sensitivity at constant

111   macro-physical condition is estimated.

112   **2. Study area and methodology**

113   2.1. Study area

114   The selected study area (Fig. 1) comprises the upper, middle, and eastern portions of the IGP. The

115   upper part consists of the densely populated and developed regions of the eastern part of Pakistan

116   i.e., Karachi (24.87ºN, 67.03ºE) and Lahore (31.54ºN, 74.32ºE) whereas the middle part comprises

117   the northern part of India i.e., Delhi (28.59ºN, 77.22ºE), Kanpur (26.51ºN, 80.23ºE), Jaipur

118   (26.91ºN, 75.81ºE), Gandhi College (25.87ºN, 84.13ºE), Kolkata (22.57ºN, 88.36ºE), Dhaka

119 (23.80ºN, 90.41ºE) and Patna (25.59ºN, 85.13ºE). The data analysis for the eastern part of IGP

120 (Kolkata, Dhaka, and Patna) is documented as supplementary materials.

Figure 1. Topography of the study area.
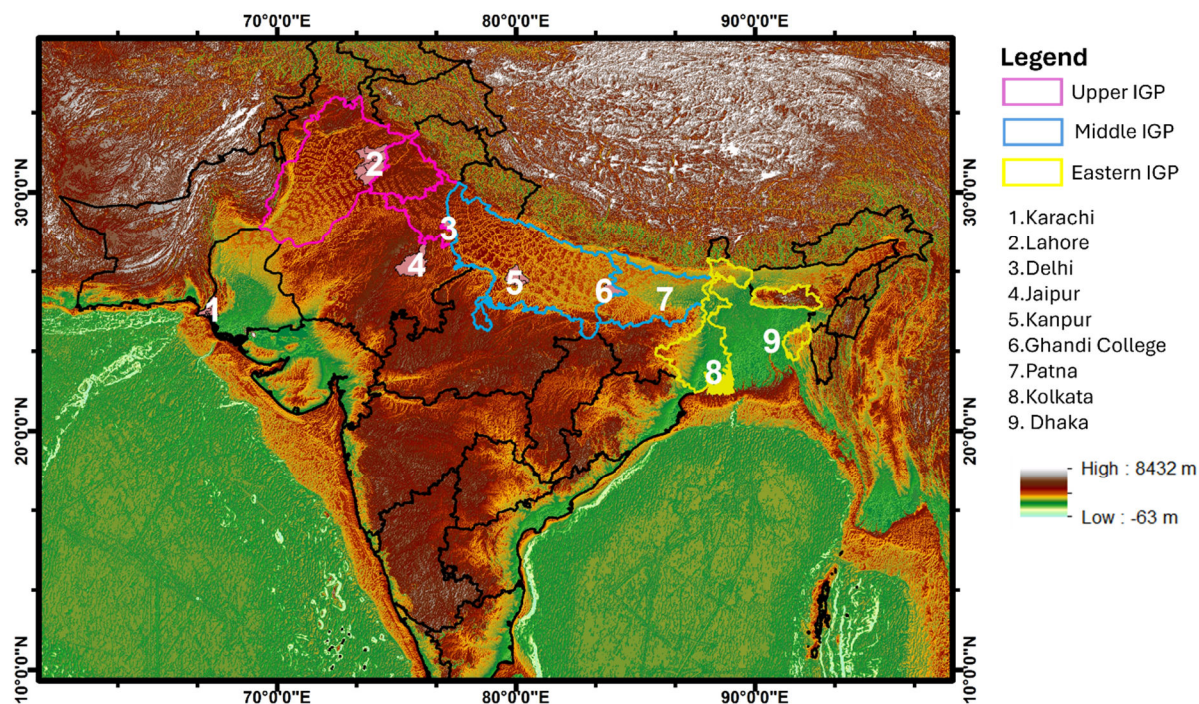
2.2. Methodology

2.2.1. MODIS, NCEP/NCAR reanalysis-II and TRMM data

125 Moderate Resolution Imaging Spectroradiometer (MODIS) is a major constituent of NASA's Earth

126 Observing System (EOS). MODIS is orbiting with two onboard satellites, Terra and Aqua,

127 launched in 1999 and 2002 respectively, with a range of 2330 km spanning the entire globe in a

128 day. It provides data and information with a spatial resolution of 1° to study atmospheric processes

129 and physical structure (Kedia et al., 2014; Srivastava et al., 2015). This study uses the daily mean

130 of combined dark target and deep blue AOD at 0.55 μm, cloud top pressure (CTP), cloud top

131 temperature (CTT), CF, CER, and COT for liquid clouds from level 3 aerosol-cloud data product

132 MOD08-TERRA. Data with AOD > 1.5 are excluded to avoid potential misidentification of

133 aerosols as clouds. The following adiabatic approximation (Brenguier et al., 2000; Wood, 2006;

134 Kubar et al., 2009; Michibata et al., 2014) is used to calculate CDNC (cm^{-3}):

$$\text{CDNC} = \left(\frac{\text{B}}{\text{CER}}\right)^3 * \sqrt[\square]{(2 * \text{CLWP} * \gamma_{\text{eff}})}$$

$$(1)$$

Where $B = \sqrt[3]{\left(\frac{3}{4}\pi\rho_{water}\right)}$ =0.0620, ρ_{water} is the liquid water density, γ_{eff} is the adiabatic gradient of liquid water content in the moist air column (Wood, 2006). Value of γ_{eff} range from 1 to 2.5×10^{-3} at a temperature of 32 K to 104 K (Brenguier, 1991; Zhu et al., 2018; Zhou et al., 2020). The CLWP is estimated by use of

$$CLWP = \frac{5\rho_w(CER)(COT)_w}{9},$$

$$(2)$$

Where, ρ_w is the water density at room temperature (Koike et al., 2016).

National Center for Environmental Prediction/National Center for Atmospheric Research (NCEP/NCAR) reanalysis datasets provide global reanalysis data sets that combine satellite observations with the simulation of models through data assimilation (Purdy et al., 2016). Daily data for meteorological parameters including temperature, RH%, and ω at 850 hPa are retrieved at a spatial resolution of T62 Gaussian grid (1.915° × 1.875°) from NCEP reanalysis-II datasets, and used to calculate lower tropospheric stability (LTS) defined as (Li et al., 2017):

$$LTS = \theta_{700} - \theta_{1000} \tag{3}$$

where θ is the potential temperature and the subscripts denote the pressure levels of 700 hPa and 1000 hPa.

The Tropical Rainfall Measuring Mission (TRMM) is the first Joint satellite mission between NASA America and National Space Development Agency (NASDA) Japan, utilizing the visible infrared and microwaves to measure the rain precipitation over tropical and subtropical regions. The main TRMM instruments that are used to measure rain precipitation are precipitation radar (PR) and TRMM Microwave Imager (TMI). Where PR is operating at a frequency of 13.8 GHz and TMI is a passive microwave radiometer consisting of nine channels. A calibrated data set TRMM-2B31 of TRMM Combined Instrument (TCI) for TRMM Multi-Satellite Precipitation Analysis (TMPA) is formed from an algorithm that uses TMI and PR. The product TMPA 3B42

162 gives the rain precipitation averages on a daily and sub-daily basis. In the current study, the data
163 product TMPA or TRMM 3B42 is used for the retrieval of PR daily. The spatial resolution of
164 TRMM 3B42 is $0.25° \times 0.25°$ and is available from the year 1998 to till date.

165   2.2.2. Methodology

166 The present study is designed to analyze and quantify the ACPI for PCs and NPCs in winter and
167 summer under a variety of meteorological conditions. The daily mean data of each parameter for
168 warm clouds are retrieved from the respective satellites and NCEP/NCAR reanalysis-II for each
169 study site. Subsequently, the VLOOKUP function in Microsoft Excel is applied to filtering out
170 counts where data is not available, searching for values of a parameter in the first column, and
171 retrieving the values of other parameters in the same rows on the corresponding dates in a large
172 dataset. The data are then segregated into two subsets for the summer and winter seasons. Based
173 on precipitation data from TRMM, the subsets are further divided into precipitating and non-
174 precipitating clouds.

175 The sensitivities of cloud parameters to CDNC are analyzed through the following formulation
176 considered from previous studies (Zhou et al., 2020):

177    $\frac{dln(COT)}{dln(CDNC)} = -\frac{dln(CER)}{dln(CDNC)} + \frac{dln(CLWP)}{dln(CDNC)}$ (4)

178 In this study, the term on the left side of equation (3) is defined as total indirect aerosol effect
179 (TIE), and the first and second terms on the right side of the equation are defined as the first indirect
180 aerosol effect (FIE), $and\ second\ indirect\ effect\ (SIE), respectively$. Similarly, the sensitivity
181 of CDNC to AOD is evaluated by employing the index of ACI:

182    $$\text{ACI}_{\text{CDNC}} = \frac{dln(CDNC)}{dln(AOD)}$$ (5)

183 The sensitivity of PR to CDNC is calculated from the following equation (Jung et al., 2012) :

184    $$S_0 = \left(-\frac{\partial ln(PR)}{\partial ln\ (CDNC)}\right)_{COT}$$ (6)

3. Results and Discussion

3.1. Regional and seasonal distribution of AOD

AOD is a commonly used proxy for aerosol concentration in the atmosphere and is analyzed here (Fig. 2-3).

IGP characteristically exhibits a diverse and massive pool of aerosols due to its unique topography. The western part of IGP is a coastal location and inlet for the westerly winds. Therefore, dry regions and the Arabian Sea in the west contribute dust, sea salt, and water vapors to the region. The Himalayas in the north act as barriers to the winds, leading to the trapping of aerosols over the central part of IGP. Therefore, this region exhibits a high concentration of anthropogenic aerosols. The Bay of Bengal in the east allows southeasterly winds to enter passing across Dhaka, Kolkata, and Patna to Delhi and Lahore (Hassan et al., 2002; Anwar et al., 2022). The westerly and easterly winds traverse forested hilly terrain, rivers, and lakes elevating humidity levels and initiating the cloud formation by activation of the newly originated small aerosol particles as CCNs and cloud formation affecting the local microclimate.

Fig. 2 shows a decadal variation in time average maps for combined dark target and deep blue AOD retrieved at 0.55 µm over the entire study area for the years (2001-2010) and (2011-2021). Also, Table 1 illustrates the percentage change in decadal averaged values of AOD. The results indicate that AOD exhibits a decrease over Karachi (-1.9%) and Jaipur (-0.5%). An increase in AOD is observed over Lahore (5.2%), Delhi (9%), Kanpur (10.7%) and Gandhi College (22.7%). Similarly, Table 1S shows the decadal change in AOD over Kolkata (18%), Dhaka (22.6%), and Patna (23.3%). Similar to Gandhi College, an increase is observed over all three areas. Reasons for the increase of aerosols include multiple sources of aerosols, human behavior, socio-economic development at local and regional levels, and unique topography for the persistence and retaining of aerosols.

Fig.3(a-b) shows the probability density function (PDF) for AOD, illustrating different distributions in the summer and winter seasons. Fig.3a shows that the distribution of AOD over Delhi, Kanpur, and Gandhi College is similar. However, a shift in the peak value of PDF towards high values of AOD over Lahore and low values over Jaipur illustrate comparatively high and low aerosol concentration in the summer season over Lahore and Jaipur respectively. Likewise, Fig.

1S shows the seasonal PDF values of AOD over Kolkata, Dhaka, and Patna. The results indicate similar seasonal distribution functions over all three areas of eastern IGP. In both seasons PDF peaks for high values of AOD are observed over Patna showing a high concentration of aerosols as compared to Kolkata and Dhaka.

The loading of high concentrations of aerosols is owing to the high density of population, industrialization, and human activities. The major sources of aerosols in all months of the year include vehicular emission originating from old transport facilities, emission of smoke and soot during consumption of biomass for cooking, heavy industrial emission, and aerosols produced in seasonal harvesting and crop residue burning. All these sources produce organic aerosols which are characterized as hydrophilic particles and have the potential to act as CCN. Likewise, the soil dust particles also act as good CCN due to their hydroscopic nature (Sun & Ariya, 2006). Moreover, the meteorological conditions also play a substantial role in enhancing AOD values such as the uplifting of loose soil dust and swelling of aerosols due to holding the water vapors (wv) for a long time (Masmoudi et al., 2003; Alam et al., 2010; Alam et al., 2011;). Also, the lower but flat PDF curve demonstrates low values of AOD over Karachi. Ali et al., 2020 associated the low AOD values over Karachi with the westerly and southwesterly wind currents at tropospheric level. However, the decreasing trend in AOD over the coastal city may also be attributed to the variations in other meteorological parameters like T and RH.

As compared to the summer season, the pattern of PDF in winter is significantly different as shown in Fig. 3b. The low value of PDF (0.5) for the high value of AOD (0.9) over Karachi illustrates a comparatively pristine atmosphere. Similarly, the PDF peaks for Lahore, Delhi, and Jaipur (0.7, 0.7, and 0.8) indicate comparatively high AOD over Delhi. Likewise, the distribution over Kanpur and Gandhi College similarly illustrates similar values of AOD (1.1 and 1.2 respectively). These high values of AOD are attributed to the high emission of anthropogenic aerosols at local and regional levels over the central part of IGP (Delhi, Jaipur, Kanpur and Gandhi College).

Few authors attributed the reduced values of AOD in the winter season to the wet scavenging and suppressed emission of aerosols from the earth surface (Alam et al., 2010; Zeb et al., 2019). However, in our case, the low (high) values in winter (summer) are associated with the dispersion of fine (course) mode particles due to the variations in meteorological conditions.
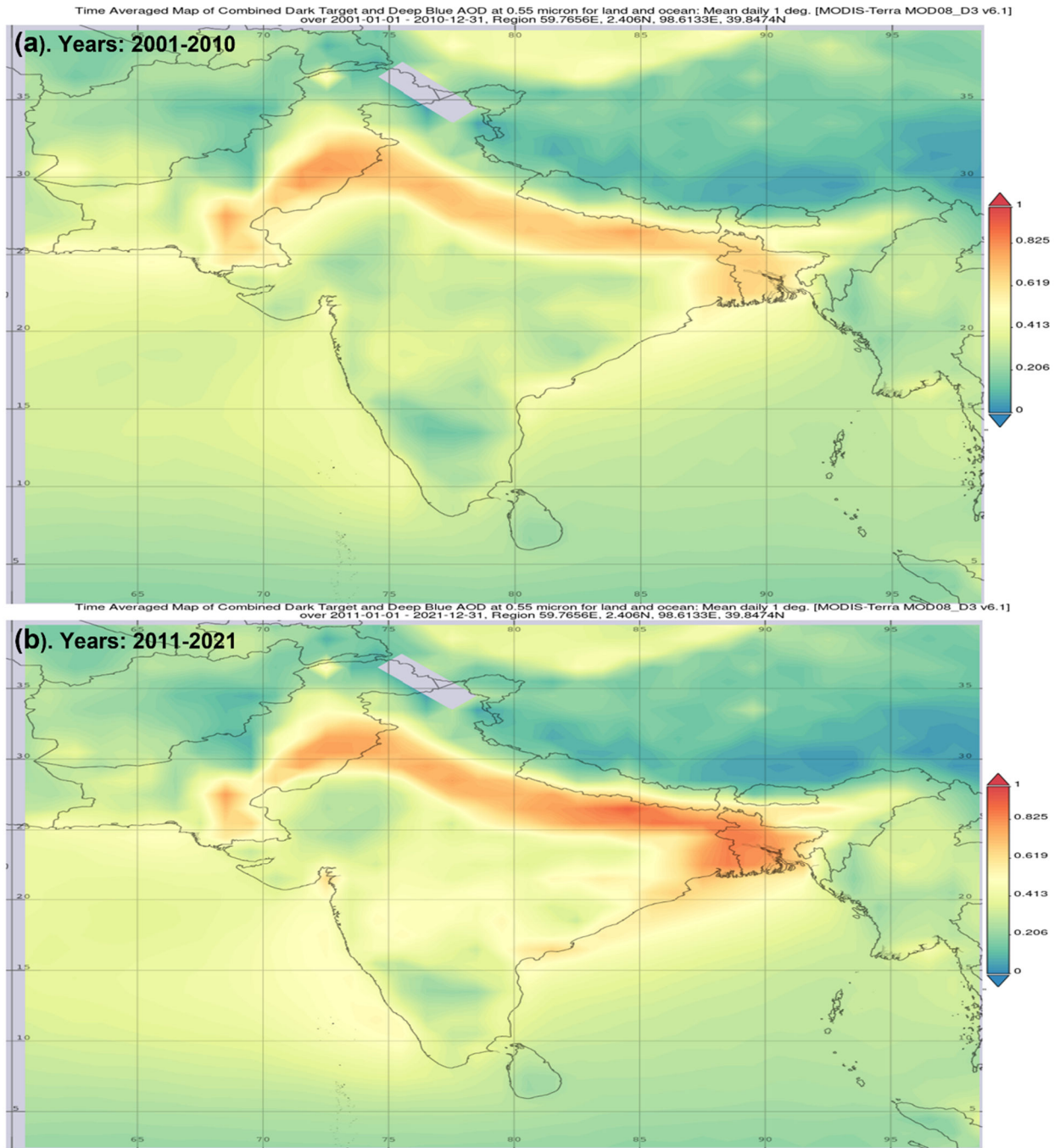
Figure 2. Decadal increase (year: 2001-2010 and 2011-2021) in AOD over study sites.

243

244

245

246

247

248

249   **Table 1.** Decadal percentage variations in average values of AOD over all study areas

	Karachi	Lahore	Delhi	Kanpur	Jaipur	Gandhi College
Total number of counts	5902	6171	5823	5201	5907	5125
Decadal change in AOD	-1.9%	5.2%	9%	10.7%	-0.5%	22.7%

250
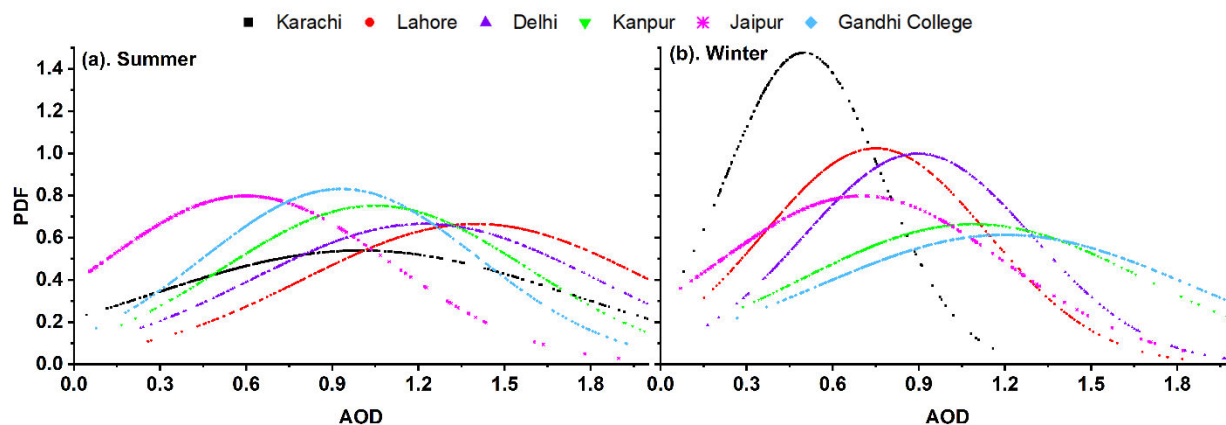
251

252   **Figure 3.** The probability density function (PDF) of AOD over study sites is shown (a) and (b) for the summer and
253   winter seasons respectively.

254   3.2. Climatology of meteorological parameters

255   Generally, LTS has relationships to factors such as temperature, humidity, wind patterns, and
256   atmospheric pressure over extended periods. It is also widely acknowledged that atmospheric
257   stability, temperature, RH wind speed, and direction play a significant role in cloud formation
258   (Yang et al., 2015; Tao et al., 2012). Therefore, the influence of long-term variations in the said
259   meteorological parameters is considered in the current study. The variations in meteorological
260   parameters have an unavoidable impact on ACPI. The parameters considered in this study include
261   the temperature, LTS to determine the lower atmospheric stability and instability that influence the
262   process of cloud and precipitation formation through its significant implications on evaporation
263   and convection of the air parcel, the RH% to estimate the level of wv and the ω to assess the
264   suitable atmospheric dynamics. Fig.4 shows the variations in LTS values for NPCs and PCs in the
265   winter and summer seasons. In the winter season, the LTS values are high for NPCs and
266   comparatively lower for PCs over entire study areas. In the summer season, the scenario is reversed
267   with high values for PCs but low values for NPCs, suggesting a stable tropospheric layer on rainy

268 days. This stabilization may be attributed to the cold pools generated by the evaporation of falling
269 rain droplets (Wu et al., 2017). The lower LTS values for NPCs in the summer season suggest the
270 likelihood of stronger instability that causes a high potential for vertical motion and the
271 development of thunderstorms. However, Karachi exhibits a distinct pattern of LTS with the
272 highest values in each case, which indicates the existence of the most stable tropospheric layer in
273 Karachi due likely to moist and cold sea breeze due to the city's coastal location.

274 The median values computed for the remaining meteorological parameters considered in this study
275 are listed in Table 2. The high values in each case are indicated in bold and the low values are
276 italicized. The results show that in the winter season, the temperature at 850 hPa (T_{850}) is relatively
277 high for NPCs ranging from 281 K to 285.6 K. The increase in RH% for PCs during winter ranged
278 from (59.5)% to (71.5)%. Also, the $\omega > 0$ for NPCs and < 0 for PCs in the winter season.

279 In the summer season, it is observed that T_{850} is comparatively higher than that for the winter
280 clouds and ranges from 298.3 to 300.2 K and 296.5 to 298.3 K for NPCs and PCs respectively.
281 The high values of T_{850} are due to intense solar fluxes in the summer season that keep the
282 temperature of the earth's surface and adjacent atmospheric layer higher. Also, the increase in
283 RH% during summer ranged between 33.5-51.7 % for NPCs. The reason for the high values of wv
284 and RH% is mainly the suitable thermodynamical conditions such as evaporation and convection
285 due to the high temperature of the earth's surface and air (Sherwood et al., 2010). The results show
286 high values of RH% 70.1% (85%) in the winter (summer) season for PCs over Gandhi College.
287 Conversely, notable fluctuations in RH% are observed over the coastal city, of Karachi, with values
288 of 71.5% (65.9%) in winter (summer). Similarly, Fig. 2S and Table 2S show the LTS conditions
289 for PCs and NPCs. The high LTS values indicate more stable conditions over Dhaka. Similarly,
290 Table 2S shows the seasonal average values for other meteorological parameters. The results
291 indicate high values of T_{850}, RH%, and ω 295.5 (297.5) K, 88.8 (83.5)%, and -0.19 (-0.17) m/s
292 respectively for PCs (NPCs) for over Patna in summer.

293 Besides, during the last two decades, the wv and fog over the Arabian Sea increased (Verma et al.,
294 2022). Therefore, the high values of wv and RH% in summer months are due to the high-speed
295 zonal winds that blow in the summer season and transport water vapors and sea salt from the
296 surface of the Arabian Sea and hydrophilic aerosols such as soil dust from deserts of Iran, Pakistan,
297 and India to IGP. Moreover, during the winter season, elevated humidity levels are noticeable over

298   IGP, particularly in the vicinity of Gandhi College. This increased humidity is a result of

299   evapotranspiration driven by agricultural practices, irrigation, the presence of rivers and lakes, and

300   the introduction of moist, cold air from western winds (Nair et al., 2020). Where $\omega < 0$ for PCs

301   over all study areas except Karachi.

302   The distinct variations in meteorological parameters reveal the occurrence of clouds with diverse

303   properties. The detailed analysis of such clouds is given in the next subsections.

304
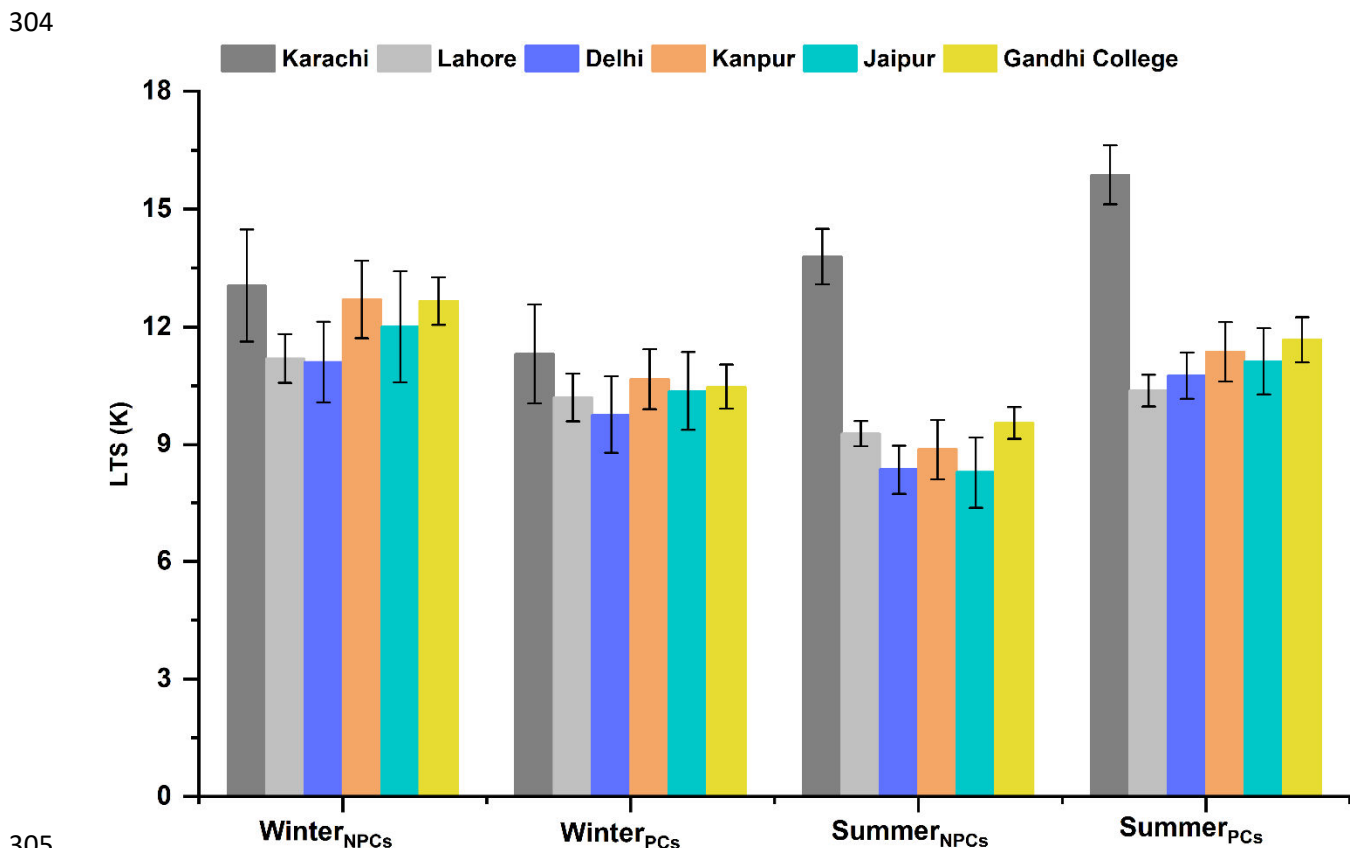
305

306   **Figure 4.** Variations in lower tropospheric stability (LTS) over all study sites for PCs and NPCs in winter and summer
307   seasons, the error bars show the standard deviation (SD) values.

308 **Table 2.** Median values of meteorological parameters for PCs(NPCs) in summer and winter seasons. Maximum values are for both types of
309 clouds shown in bold and minimum values are indicated in italics.

	Winter Season			Summer Season		
	T_{850} (K)	RH%	ω (m/s)	T_{850} (K)	RH%	ω (m/s)
Karachi	**284.6 (285.8)**	**71.5** (38)	-0.038 (*0.030*)	*295.9* (298.8)	65.9 (45.9)	*0.005* (-0.003)
Lahore	*280.5* (*281.2*)	*59.5* (35.5)	*-0.02* (**0.065**)	**298.3 (300.2)**	65 (*33.5*)	*-0.028* (*0.025*)
Delhi	284.2 (283.1)	60.2 (*33.8*)	**-0.1** (0.04)	296.5 (299.4)	64.2 (42)	*-0.05* (*-0.001*)
Kanpur	283.8 (284.1)	65.7 (36)	**-0.1** (0.048)	296.5 (298.4)	73.7 (43.6)	*-0.13* (-0.08)
Jaipur	283.9 (284.1)	66 (40.5)	-0.065 (0.049)	296.8 (298.7)	*64* (**51.7**)	*-0.04* (*-0.029*)
Gandhi College	283.2 (284.1)	70.1 (**45.7**)	**-0.1** (0.05)	296.9 (*298.3*)	**85** (42.5)	***-0.16*** (***-0.11***)

310

311

312

313

314

3.3. Regional and seasonal distribution of clouds and precipitations

3.3.1. Regional and seasonal differences in cloud occurrence and its microphysical structure

Fig.5 shows the frequency of occurrence of precipitable clouds and the total number of cloudy days. Chen et al. (2018) suggested the COT to be an effective measure for assessing the clouds and potential for precipitation. In our case, to avoid any overestimation, the COT data are aligned with PR data on corresponding dates and then filtered to include COT ~ > 5 for PCs. The results show that in the winter season, the frequency of clouds is low over Karachi and high over Lahore and Gandhi College. The results suggest the high number of PCs only over Lahore. In the summer season, a high number i.e., 74 % of the total data counts over Gandhi College are identified as cloudy days, 60 % of which are PCs. Similarly, most of the clouds over Lahore, Delhi, and Jaipur are PCs. Conversely, the least number of PCs (6 %) are found over Karachi. Likewise, Fig. 3S shows the total number of cloudy days and the number of days on which PCs occurred. The high occurrence of clouds is observed over Kolkata 83% (60%) and Dhaka 91% (69%) in the summer (winter) season. The high occurrence of PCs in summer is due likely to the significant impact of elevated aerosols with the southwesterly winds on the summer monsoons and the occurrence of PCs. Therefore, Kolkata and Dhaka are of critical importance from the perspective of aerosol loading and ACI (Dahal et al., 2022).

334

335
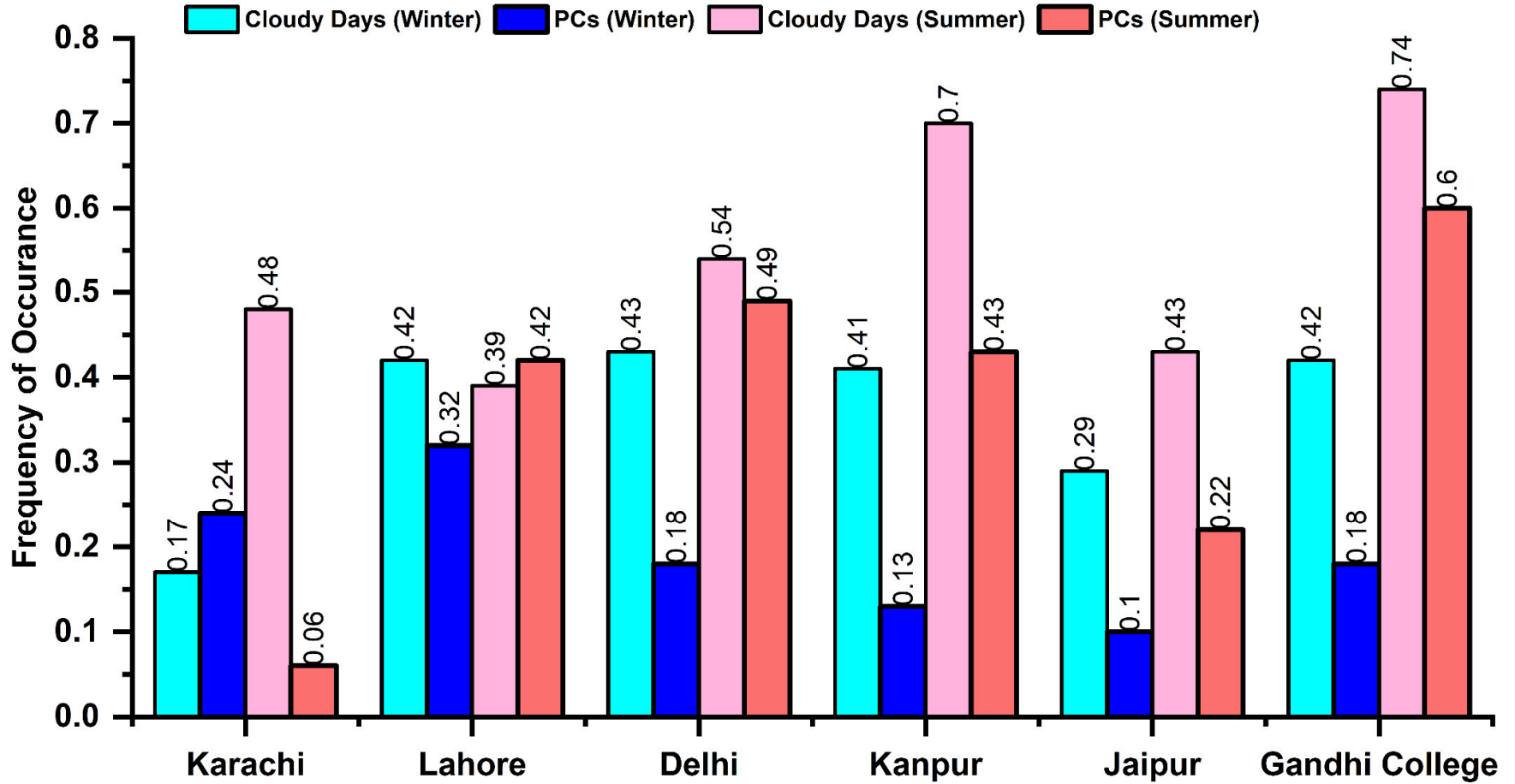
Figure 5. The frequency of occurrence of total cloudy days (including PCs and NPCs) and only PCs is shown for both winter and summer seasons.

337   Table 3 shows the criteria adopted from previous papers (Rossow & Schiffer, 1999; Wyant et

338   al., 2006; Sharma et al., 2023) for further classification of NPCs and PCs into different types

339   of clouds. The aim of identifying the cloud types is to assess the cloud regimes and their vertical

340   structure for a better understanding of ACPI. Following table 3, Fig. 6 shows joint histograms

341   of COT-CTP displaying the median values of CF for nine different types of clouds. For a quick

342   visual comparison, the cloud types are ordered from low to high-level clouds. Also, for each

343   histogram, the bins of COT and CTP are located on the x- and y-axis respectively. The CF of

344   each bin is represented with the colored bar with its value mentioned in the histograms as shown

345   in Fig. 6.

346   The results exhibit noticeable differences in the pattern of cloud regimes over all study areas.

347   The diverse CF values are observed in the winter and summer seasons for NPCs and PCs over

348   Karachi. In the winter season, only stratus NPCs (23 < COT <60, 800 > CTP > 680 hPa) are

349   dominant with CF ~ 0.9. While, in summers, the high value of CF ~ 0.9 for low and

350   intermediate thickness of high-level clouds such as Cirr-Stratus NPCs (3.6 < COT < 23, 180<

351   CTP < 440 hPa) are observed. Similarly, the types of PCs in both summer and winter seasons

352   that occurred with CF ~1.0 include cirrus and cirrus-stratus. The relatively reduced value of CF

353   for thick NPCs in winter and PCs in summer is attributed to the low values of AOD and high

354   values of LTS. The results depicted slight differences and similarities in CF values for thick

355   and thin NPCs respectively in the winter season for all areas except Karachi. Besides, the high-

356   level PCs are identified in the two bins of CTP (180< CTP < 440 hPa) and (440< CTP < 680

357   hPa) over all study areas. The formation of these similar types of PCs in winter is associated

358   with the similarities in ω, LTS values, and aerosol concentration.

359   Likewise, in the summer season, the matrices of PCs and NPCs exhibit a wide range of cloud

360   types. However, the CF values are comparatively high for PCs. Most of the identified PCs are

361   formed in the two bins of CTP (180< CTP < 440 hPa) and (440< CTP < 680 hPa) with CF

362   values ranging from 0.8 to 1.0. The results suggest low values of CF for the low-lying thick

363   NPCs over all study areas. Moreover, the results illustrate a more frequent occurrence of all

364   three types of thick NPCs in one bin of COT (23 < COT< 60) and all the three types of high-

365   level NPCs for CTP (180 < CTP < 440 hPa) over Delhi, Kanpur, and Gandhi College.

366   Therefore, these are considered the cloudiest regimes. Besides, contrasting regional variations

367   are also observed in PCs. The maximum CF values for all types of PCs are observed over

368   Kanpur and Gandhi College. Similarly, relatively good values of CF in a bin of COT (23 <

COT< 60) and a bin of CTP (180 < CTP < 440 hPa) over Lahore, Delhi, and Jaipur depict the frequent occurrence of thick and high-level PCs respectively. In addition, among all the estimated low-level PCs, cumulus and strato-cumulus exhibit good CF values (0.7) over Kanpur and Gandhi College. The formation of thick clouds can be attributed to the enhanced convection process due to atmospheric instability.

Table 3. Classification of clouds based on CTP – COT joint histograms.

CTP (hPa)	COT		
	0-3.6	3.6-23	23 to >60
440 to <180	Cirrus	Cirr-Stratus	Deep convection
680-440	Alto-Cumulus	Alto-Stratus	Nimbo-Stratus
<800 to 680	Cumulus	Strato-Cumulus	Stratus
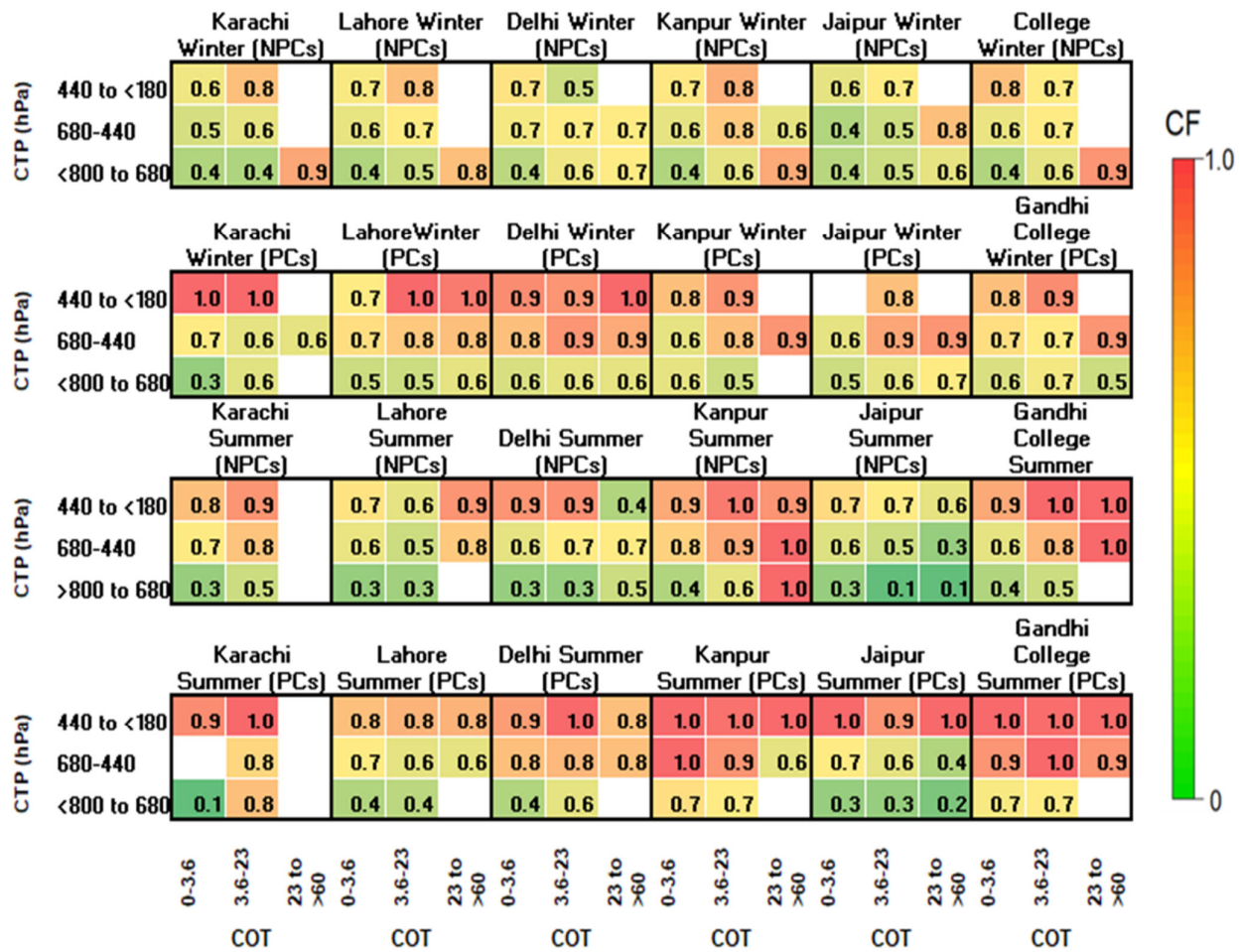
Figure 6. Types of NPCs and PCs in winter and summer season

377

378

379   After estimating the cloud types, Fig. 7 shows the probability distribution function (PDF) of

380   cloud microphysical properties for the identification of differences in the microstructure of

381   NPCs and PCs in the summer and winter seasons. From the results, it is depicted an

382   approximately similar pattern for the CER of NPCs in winter. However. the clouds have high

383   peaks of PDF for lower values of CDNC over Karachi. The low number of CDNC results in

384   thin NPCs as shown in Fig.7. Similarly, Fig. 7(c and g) shows the microstructure of NPCs in

385   summer. The results indicate that as compared to CER values in winter, the probability of CER

386    $>\sim$15 µm is high in the summer season. However, the high peak for CER < 15 µm is observed

387   over Karachi. Similarly, the CDNC shows a high probability for CDNC > 50 cm^{-3} with high

388   PDF values over Karachi. Where the lowest number of CDNC is observed over Lahore

389   indicating the formation of high-level thin NPCs in summer.

390   Fig. 7(b and f) shows the distribution pattern of CER and CDNC of PCs in the winter season.

391   It is observed that the distribution of CER for PCs is like that for NPCs in the winter season.

392   However, PDFs have peak values for relatively higher CDNC, which illustrates the occurrence

393   of thick clouds. Fig. 7(d and h) shows the variations in CER and CDNC in the summer season.

394   The results show a wider distribution for CER > ~15 µm and higher peaks for CDNC > ~ 50

395   cm^{-3} suggesting the formation of thick PCs in summer as shown in Fig.6.

396

397
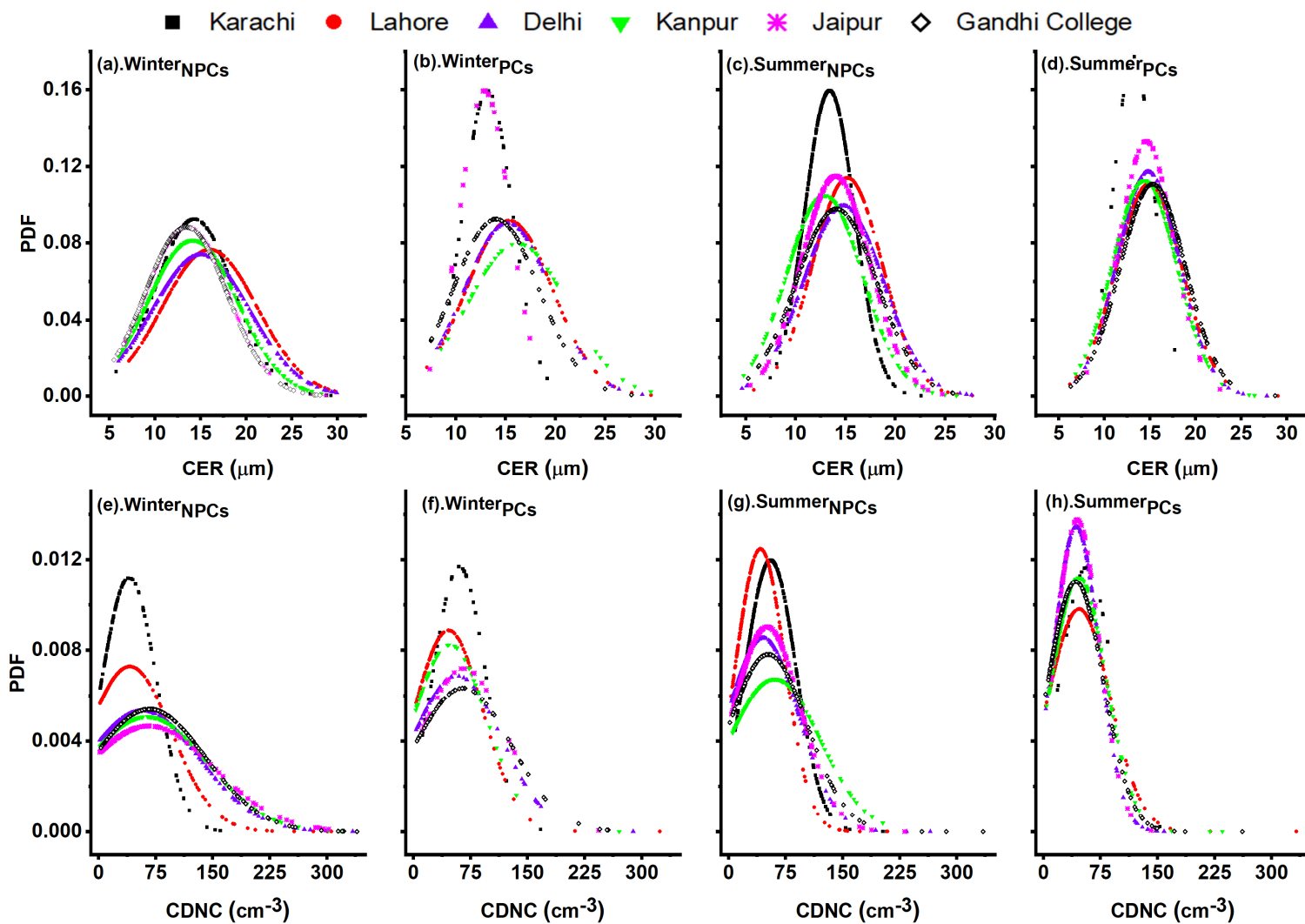
Figure 7. Probability density function (PDF) of precipitating (PCs) and non-precipitating clouds (NPCs) in the winter and summer season

3.4. Aerosol-Cloud-Precipitation Interaction (ACPI)

In the following sections, ACPI is analyzed and discussed in detail for PCs and NPCs in the summer and winter seasons.

3.4.1. Aerosol effects on cloud properties

The impact of aerosols on CDNC and CER of PCs and NPCs is illustrated as scatter plots in Fig. 8-9. The quantification of the AOD-CER and AOD-CDNC relationships is demonstrated through detailed linear regressed slopes, regression coefficients (R^2), and Pearson's correlation coefficient (R). The color bar represents the variations in LTS. The results show that the two-sample student's t-test is carried out to analyze the AOD-CER and AOD-CDNC relationship in view of statistics. The results illustrate that the relationships are statistically significant at a 95% ($p < 0.05$) significance level for all study areas. Fig.8 shows that in the winter season, the AOD-CER correlation is good for PCs and weak for NPCs. The results also show that the LTS values are higher for NPCs. The weak AOD-CER correlation may be linked to the inhibition of droplet growth due to less soluble aerosols, originating from biomass burning (Kang et al., 2015). In our case, all the selected study areas are among the most urbanized and industrialized areas of IGP. Therefore, most of the prevailing aerosols are the less soluble soot and BC particles. That weakened activation of cloud droplets inhibits the formation of PCs and evaporates to higher altitudes thereby increasing the droplet residence time (Kumar & Physics, 2013). Besides, the results show a contrasting pattern of LTS values. Although RH over Karachi (38.3±9 %) is higher than over the other study areas (shown in Table 2), the negative AOD-CER correlation is observed over Karachi due to its coastal location, the low value of AOD and high level of LTS.

Fig. 9 illustrates the AOD-CER and AOD-CDNC correlation in the summer season. The results depict a more significant and positive AOD-CER correlation in the summer season than winter season. Unlike the winter season, high LTS values are observed for PCs. Yuan(2008) associated the positive AOD-CER correlation with the soluble organic aerosols. Myhre et al. (2007) hypothesized that the positive AOD-CER correlation is a maximum for low CTP and a minimum for high CTP. Hence, in our study, referring to the approximated CF values shown in Fig.6, the significant and positive AOD-CER correlation under unstable atmospheric conditions resulted in thick and high-level clouds. Furthermore, it is observed that CER and CDNC values for NPCs increase with increasing instability. Meanwhile, the enhanced process of droplet activation may result in large AOD, higher CER, giant, and fewer CCN (Yuan, 2008).

432 Therefore, the weak correlation of AOD with CER and CDNC may be due to the
433 anthropogenically ejected water-soluble organic aerosols and a smaller number of CCN.

434 Fig. 5S and 6S show the impact of AOD on CER and CDNC for PCs and NPCs in winter and
435 summer respectively. The results indicate a positive and weak AOD-CER correlation of 0.2,
436 0.07, and 0.004 for NPCs over Kolkata, Dhaka, and Patna respectively, and for PCs (0.08) over
437 both Kolkata and Patna. Similarly, a positive and weak AOD-CDNC is observed over all areas
438 for PCs. Likewise, Fig. 6S also illustrates weak AOD-CER correlation is 0.06, 0.2, and 0.12
439 for both types of clouds in summer. As compared to other areas, the correlation analysis is less
440 significant over Karachi, Kolkata, Dhaka, and Patna. This can be attributed to the persistence
441 of diverse aerosol types influenced by their coastal locations, different meteorology, and the
442 alternating inflow and outflow of easterly and westerly winds.

443 Recent advances in remote sensing led to cost-effective solutions and an increase in available
444 data at various temporal and spatial resolutions to bridge scientific gaps among different
445 disciplines. While satellite-based retrievals have many advantages over in-situ and ground-
446 based measurement such as broader regional coverage and enhanced spatial resolution, they
447 are still prone to considerable uncertainties owing to the indirect nature of remote-sensing,
448 retrieval algorithms, thermal radiance, infrequency of satellite overpasses, and cloud top
449 reflectance (Hong et al., 2006; Tian et al., 2010; Hossain et al., 2006). In our study, apart from
450 the aforementioned factors contributing to the uncertainty, any residual cloud contamination
451 could also lead to biased retrieval of AOD. Likewise, satellite-based retrievals for cloud
452 properties are crucial to understanding the pivotal role of clouds in climate and the role of
453 clouds is still a dominant source of uncertainty in the prediction of climate change. These,
454 uncertainties in AOD and retrievals of cloud properties also propagate through the modeling
455 process, potentially leading to less accurate climate predictions. Likewise, these uncertainties
456 appeared to influence the findings in the current investigation. For instance, a limited
457 correlation between AOD and CER is observed over Lahore, particularly in cloudier regimes
458 as depicted in Fig. (5-6). This contrasts with robust impacts documented in earlier studies
459 (Michibata et al., 2014). However, high sensitivity of SIE is observed for PCs particularly in
460 the winter season indicating the delay in the onset of precipitation and more retention of clouds.
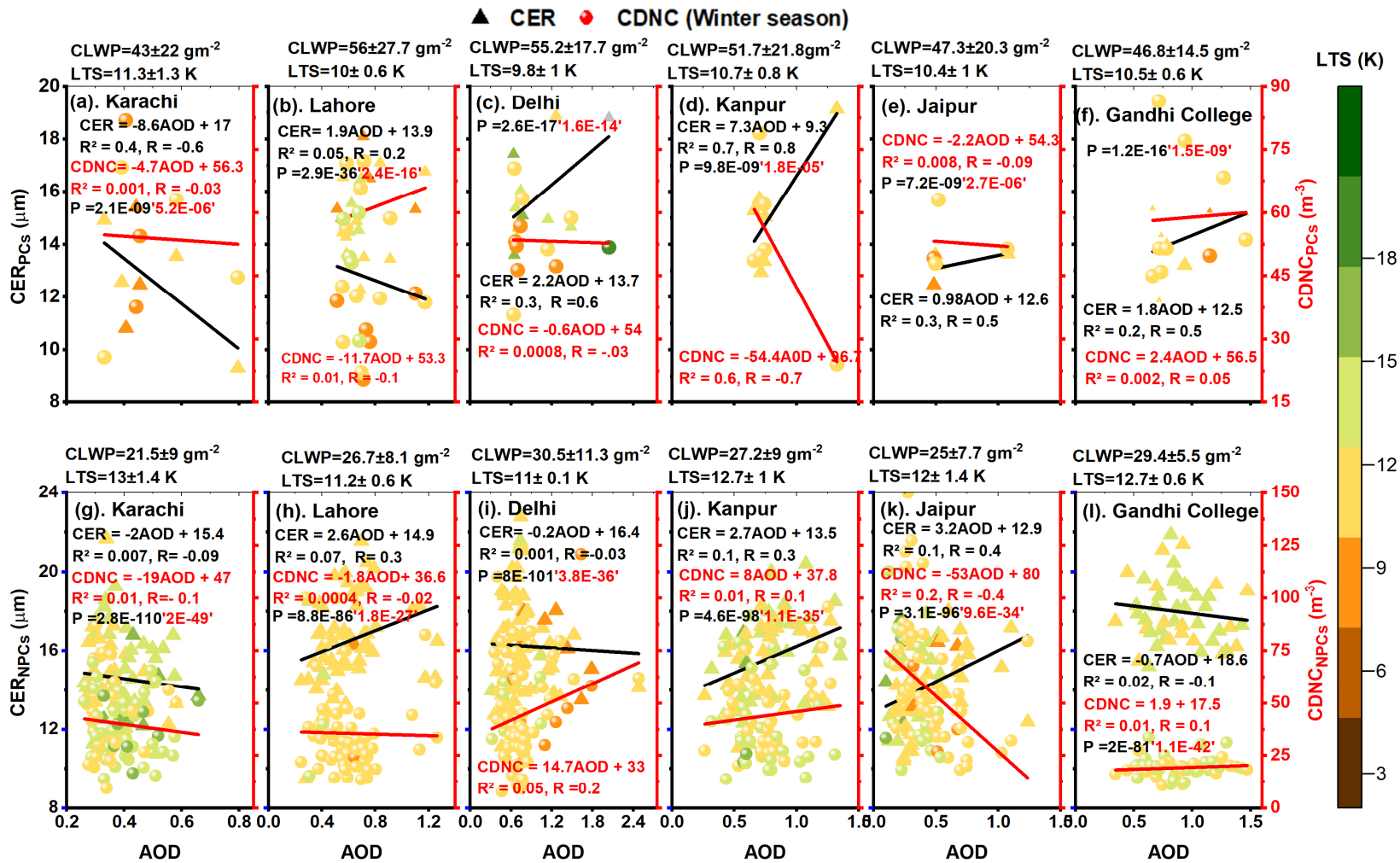
Figure 8. AOD-CER and AOD-CDNC regression and correlation coefficient considered at 95% confidence level for PCs and NPCs over all study areas in the winter season.
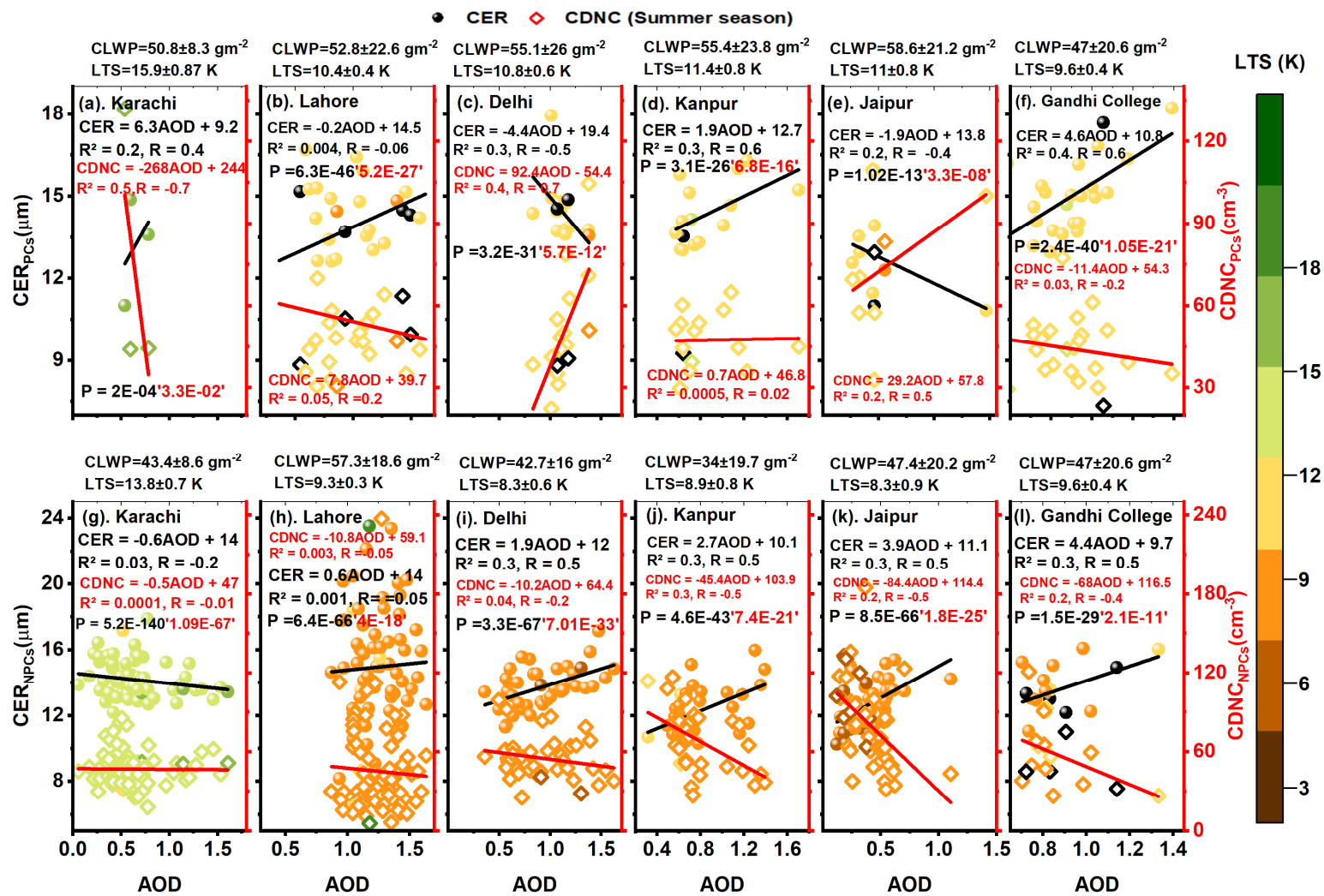
Figure 9. Same as Fig. 8 but in the summer season.

464

465

 3.4.2. Seasonal variations in sensitivities of aerosol-cloud indirect effects and ACI

467 Fig.10 shows an assessment of four ACI sensitivities in terms of CDNC using daily mean

468 values of MODIS observations available over the entire study area. Studying the effects of

469 aerosols on the co-located clouds is a challenging task due to the overestimation of thin clouds

470 in AOD retrievals. Therefore, to minimize the propagation of AOD retrieval errors in ACI, the

471 current study attempted to estimate the sensitivities of different cloud mechanisms to CDNC.

472 The sensitivity of CER to CDNC is assessed as a signature of FIE as shown in Fig.10a. The

473 positive values illustrate that CER decreases with an increase in CDNC revealing the

474 occurrence of the Twomey effect. While the negative values depict the anti-Twomey effect.

475 Tripathi et al., (2007) divided IGP into four regions western, central, eastern part of IGP, and

476 the foothills of the Himalayas. Their results depicted a high concentration of dust in the western

477 part, and an increase in anthropogenic aerosols as one moves from the western to the eastern

478 part of IGP. Therefore, they attributed the resulting strong indirect effect in winter to the high

479 concentration of regional anthropogenic pollution. However, in our case, the FIE is investigated

480 for both PCs and NPCs in both seasons. The resulting approximations in the winter season

481 show strong (weak) sensitivity of FIE for PCs (NPCs). Similarly, the estimated sensitivity of

482 FIE for all NPCs and PCs is also positive in the summer season. Fig. 7S(a) shows sensitivities

483 for FIE in both seasons for PCs and NPCs. The results indicate high values of sensitivity FIE

484 in the winter season which is similar to the results for Karachi, Lahore, Delhi, and Kanpur as

485 shown in Fig. 10 a. This is attributed to high levels of aerosol emission from residential heating

486 and industrial activities. Furthermore, the results illustrate higher values of FIE in summer. This

487 is attributed to the massive aerosol loading due to aerosol carried by winds and originating

488 from anthropogenic activities and unstable meteorology.

489 Fig. 10b illustrates the sensitivity of CLWP to CDNC as a proxy for the evaluation of the SIE

490 or lifetime effect. The positive sensitivity estimated for all NPCs and PCs suggested that the

491 CLWP increases with an increase in aerosol. Further, the results show that the sensitivity of

492 SIE is stronger for PCs in winter which indicates the delay in the onset of high PR. Similarly,

493 the results show that the SIE sensitivity values are higher for PCs than for NPCs in the

494 corresponding seasons. Therefore, the results depict that the lifetime of PCs is greater than

495 NPCs. This is attributed to the high level of RH for PCs as shown in Table 2. Fig. 10 (a and b)

496 shows that the FIE sensitivities are weaker than SIE.

497   Fig. 10c shows the TIE in terms of the sensitivity of COT to CDNC. The results illustrate

498   positive values of sensitivity for all NPCs and PCs which indicate that COT increases with an

499   increase in aerosol concentration. The results also reveal that the sensitivity of TIE is a linear

500   sum of the sensitivities of FIE and SIE. Further, the results also suggest that the variations in

501   TIE sensitivity are largely dependent on SIE.

502   Fig.10d shows the sensitivity of CDNC to AOD as an estimation of ACI in terms of CDNC.

503   The positive values show the increase in CDNC with the increase in AOD. Therefore, positive

504   ACI reflects the inhibition of precipitation formation. Whilst, the negative values illustrate the

505   decrease in CDNC and enhanced PR (Fan et al., 2018). The results depicted relatively large

506   and positive sensitivities for NPCs in winter over Lahore, Delhi, and Kanpur, which inhibits

507   the onset of rainfall. The Sensitivity of ACI for NPCs in summer is positive over Karachi and

508   Lahore and negative over Delhi, Kanpur, Jaipur, and Gandhi College. Ackerman et al. (2004)

509   associated the negative ACI_{CDNC} with the wet scavenging and mixing of air by entertainment.

510   In our case, negative ACI may be due to the growth of CER and a decrease in CDNC with

511   aerosol loading under unstable conditions(shown in Fig. 9). Further, the magnitude of

512   sensitivity for PCs in summer is low. This can be due to the droplet growth through collision

513   coalescence and wet scavenging in thick clouds, decreased dependency on CCN.

514

515
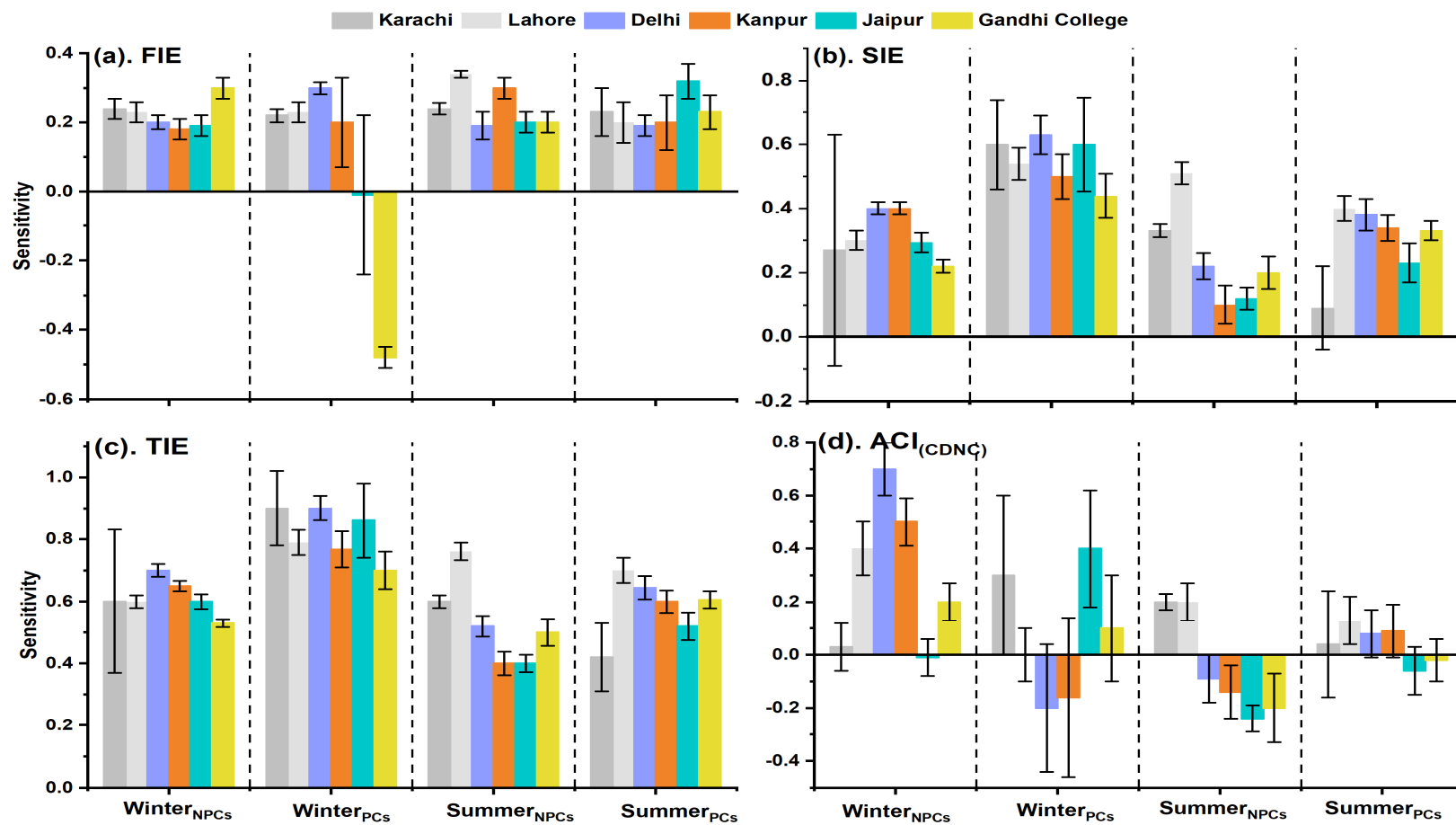
Fig. 10. The sensitivity matrices estimated for an aerosol-cloud relationship using CDNC are shown in (a) FIE $= -\left(\frac{\partial ln\,(CER)}{\partial ln\,(CDNC)}\right)$ (b) SIE $= \left(\frac{\partial ln\,(cLWP)}{\partial ln\,(CDNC)}\right)$, (c) TIE $= \left(\frac{\partial ln\,(COT)}{\partial ln\,(CDNC)}\right)$ and (d) ACI $= \left(\frac{\partial ln\,(CDNC)}{\partial ln\,(AOD)}\right)$. Where the error bars show the standard deviation (SD).

519   *3.4.3. Aerosol effects on precipitation*

520   Fig. 11 shows the average values of PR in mm/day retrieved from TRMM. The results show

521   an obvious seasonal difference in precipitation occurrence. The reason for the high (low) PR

522   values is due to the suitable meteorological conditions including high (low) LTS values for PCs

523   in the summer (winter) season (shown in Fig. 8-9). The stable atmospheric condition with a

524   high LTS value in winter serves to inhibit the convection process and have a significant impact

525   on controlling the PR in winter (Zhao et al., 2006). Conversely, during the summer season,

526   meteorological instability prevails with low LTS values which result in high RH. This not only

527   causes enhanced AOD due to the water uptake and results in swelled hydrophilic aerosols

528   (Alam et al., 2010; Alam et al., 2011) but also affects the cloud and precipitation formation due

529   to the enhanced evaporation and convection. Additionally, Fig. 8-9 also shows evidently and

530   specifically during summer that the possible cause of positive AOD-CER correlation is the

531   negative AOD-CDNC correlation under unstable meteorology over all areas except Karachi.

532   As a result, Fig. 11 shows high (low) values of PR over all areas with a maximum over Gandhi

533   College (Karachi). The results show a high (low) approximation of PR over Gandhi College

534   (Karachi). Knowing that the rate of conversion of CDNC to precipitation is proportional to

535   CER (Wolf & Toon, 2014). Therefore, the high PR values are due to the growth of bigger cloud

536   droplets in summer. Further, apart from the reasons mentioned in the preceding sections, the

537   other justification for the differently perturbed aerosols, clouds, and precipitation pattern over

538   the study areas in summer is due to the entrance of southeast winds from the Bay of Bengal

539   passing across Gandhi College to Delhi and Lahore and the entrance of same winds from

540   Arabian sea to Pakistan through Karachi (Anwar et al., 2022).

541   Fig. 12 shows scatter plots of PR versus CDNC. The plot is colored with COT to examine the

542   impact of CDNC on PR for similar macrophysics. When CDNC is less, then the COTs are

543   sparse grow larger, form less reflective clouds, and precipitate faster (Kump & Pollard, 2008).

544   The same phenomenon seems true in our case. The results illustrate high PR (0.0007 mm/day)

545   values for clouds with COT ranging from 3 to 28 with CDNC $< \sim 50$ cm^{-3} and intermediate for

546   optically thick clouds and CDNC $> \sim 50$ cm^{-3} in both seasons.

547
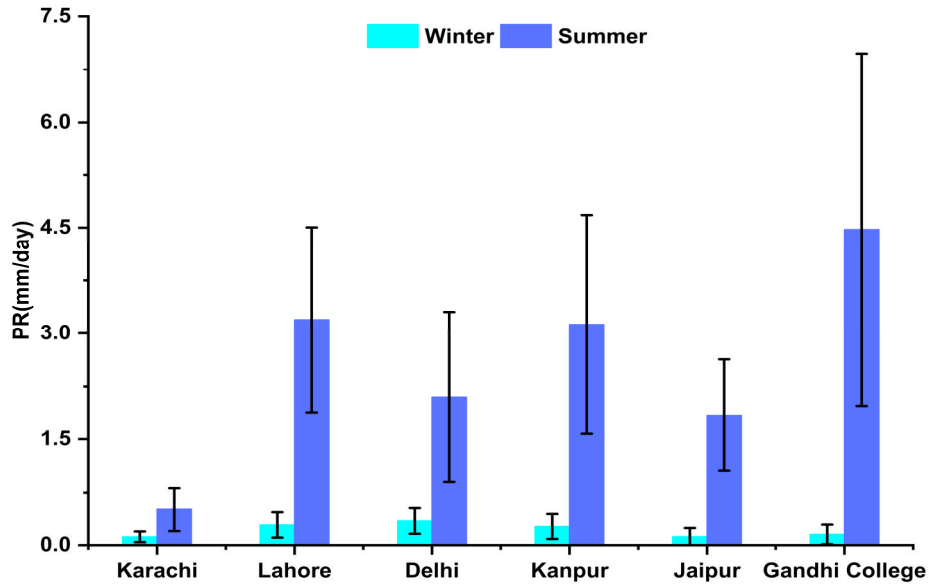
Figure 11. Mean Precipitation rate (PR) for the PCs in winter and summer season and SD
values with a 95% confidence interval.

548
549
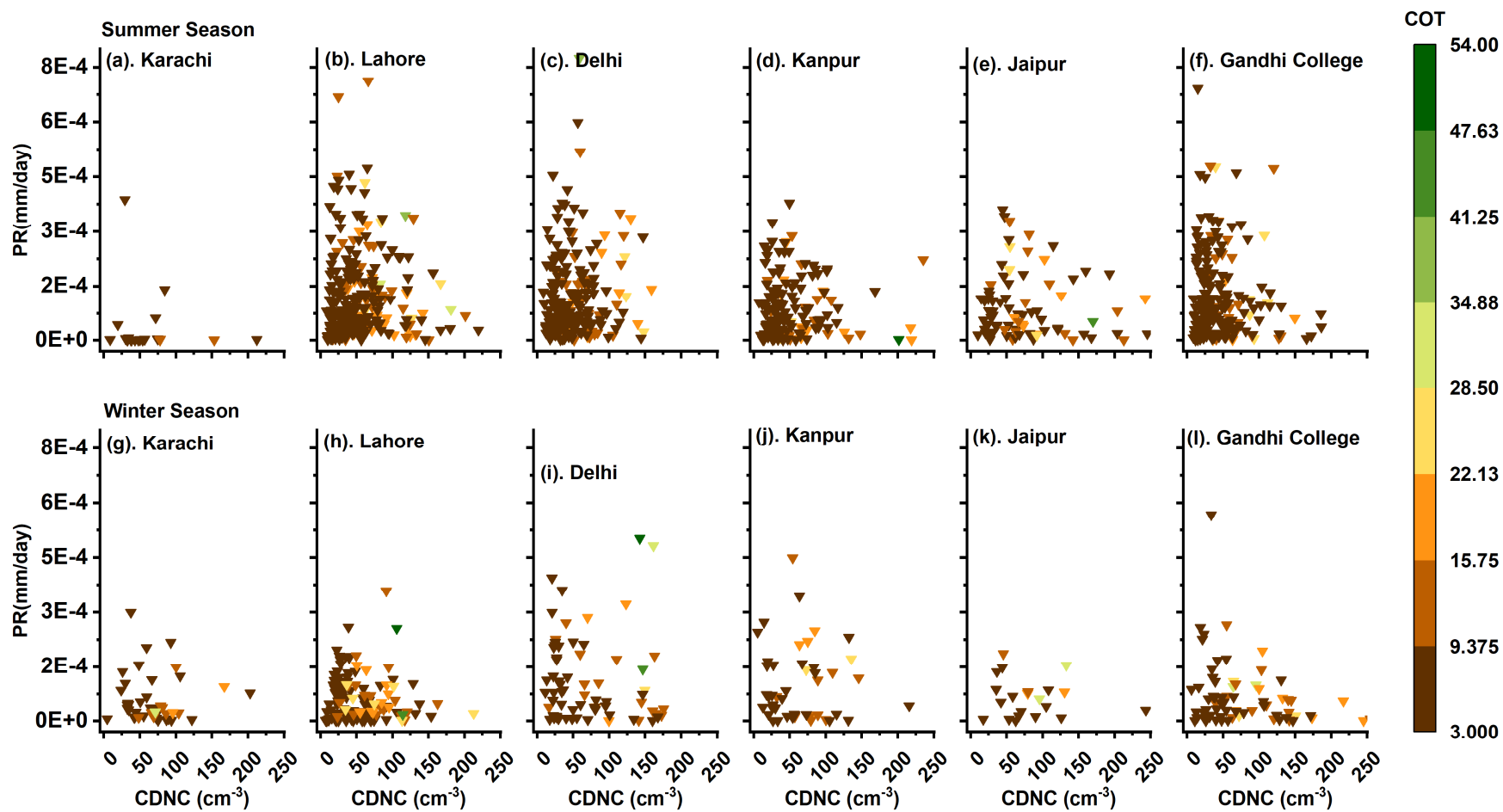
Figure 12. Scatter diagrams of PR (mm/day) versus CDNC (cm⁻³) in summer and winter seasons. color coding shows the COT of PCs.

553   Fig.13 shows the sensitivity (S_o) of PR to CDNC defined by $S_o = \left(-\dfrac{dln(PR)}{dln\,(CDNC)}\right)_{COT}$ for clouds

554   of low and intermediate thickness illustrated in Fig. 13 a and Fig. 13 b respectively. However,

555   sensitivity analysis for COT > 23 could not be performed due to the smaller number (0 to 04)

556   of available samples. In the sensitivity equation, the minus sign shows the suppression of

557   precipitation formation due to the increase in CDNC. Further, when S_o is positive, the

558   correlation between PR and CDNC is negative; however, for negative S_o, PR and CDNC are

559   positively correlated. The results show peak values of S_o i.e., 0.7 ± 0.3, 0.6 ± 0.3, 0.5 ± 0.3, and

560   0.4 ± 0.4 over Jaipur, Delhi, Gandhi College, and Karachi respectively at intermediate values

561   of COT in winter, indicating the occurrence of lightly precipitating clouds. Referable to Fig.

562   13b, the low magnitude of S_o 0.2 ± 0.3 and 0.08 ± 0.2 over Kanpur and Lahore respectively is

563   due to coagulation, in which precipitations are less sensitive to CDNC.

564
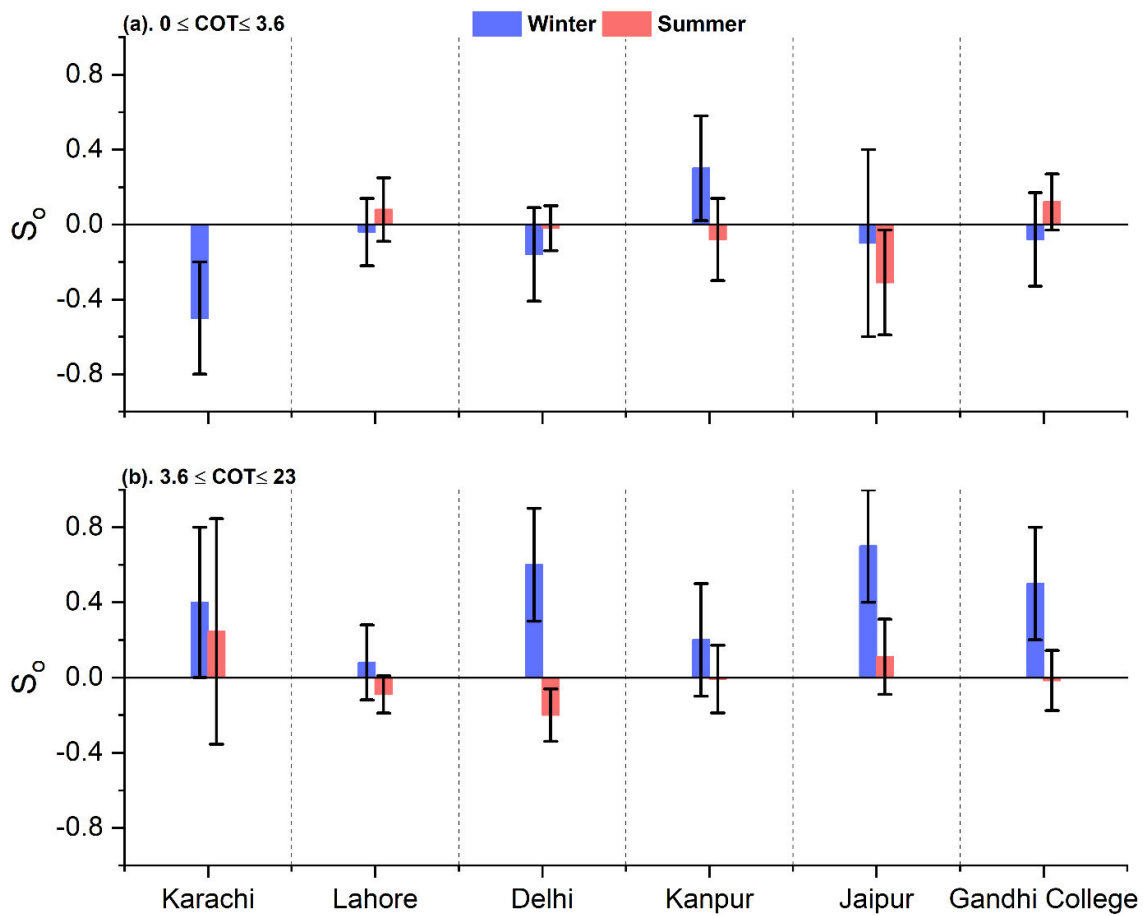
565

566 **Figure 133.** The sensitivity 'So' of precipitation rate (PR) for two bins of COT is shown in (a).
567 $0 \le COT \le 3.6$ and (b). $3.6 \le COT \le 23$.

568

4. Conclusion

In this study, the long-term (2001-2021) data retrievals from MODIS coupled with TRMM and NCEP/NCAR reanalysis-II datasets over the entire study area are compiled and analyzed for PCs and NPCs in the winter and summer season. The following are the main findings of this study.

A decadal decrease in AOD is observed over Karachi (-1.9%) and Jaipur (-0.5%). Meanwhile, AOD exhibits an increase over Lahore (5.2%), Delhi (9%), Kanpur (10.7%) and Gandhi College (22.7%). The LTS values are High (low) for NPCs (PCs) in winter and for PCs (NPCs) in the summer season. However, among all study areas, Karachi exhibits comparatively high LTS values in both seasons. Apart, the increase in RH% for PCs ranged from 33-57% in winter and from 25-45 % in summer. $\omega > 0$ for all NPCs in winter and < 0 for PCs in both winter and summer seasons.

In the winter season, a low frequency of cloudy days over Karachi and a high over Lahore and Gandhi College is estimated. Also, the high number of PCs is estimated only over Lahore. In the summer season, out of the 74 % of the cloudy days, 60 % are PCs over Gandhi College. Similarly, most of the clouds over Lahore, Delhi, and Jaipur are PCs. Conversely, the lowest number of PCs (6 %) is found over Karachi. The high-level PCs are identified in one bin of CTP (180< CTP < 440 hPa) over all study areas in winter. In the summer season, all three types of high-level and thick PCs have significant values of CF. The low-level PCs are identified as stratus clouds. Further, PDF values for CER $> \sim 15$ μm and CDNC $> \sim 50$ cm^{-3} for NPCs and PCs are high (low) in summer (winter) over all areas except Karachi.

The AOD-CER correlation is good for PCs and weak for NPCs in the winter season. Also, the CER and CDNC values increase with the increase in LTS. The sensitivity value of FIE is high (low) for PCs (NPCs) in winter. Further, the magnitude of sensitivity of FIE (SIE) is low (high). Also, the sensitivity of TIE is a linear sum of the sensitivities of FIE and SIE. Further, ACI sensitivity values for PCs in summer are small, illustrating less dependency of CER on CDNC in thick clouds.

The high (low) PR values are observed in summer (winter). Further, high PR values for comparatively thin clouds with fewer CDNC $< \sim 50$ cm^{-3} and intermediate for optically thick clouds and CDNC $> \sim 50$ cm^{-3} are observed. Sensitivity values are small (high) for thick clouds in summer (winter).

Being one of the major source regions of anthropogenic aerosols across the globe, IGP offers interesting insights into the study of ACPI coupled with aerosol indirect effects. This study highlights that the aerosol-cloud relationship exhibits different behavior under different meteorological conditions, at coastal and inland locations. Thus, compared to other study areas, the stable atmospheric conditions due to the constant sea breeze weakened the ACI over Karachi, which resulted in a smaller number of CDNC, NPCs, and PCs. Further, our study also provides a very good platform for the detailed analysis of sensitivity tests of aerosol indirect effects and precipitation formation.

Limitations and future recommendations:

Although the current study is as thorough as possible, however, it has its limitations due to the topographical complexity of IGP, the lack of in-situ measuring instruments in Pakistan, and the intrinsic uncertainties associated with satellite-based data. Therefore, simulations of ground-based measurements along with satellite-based retrievals and calculation of cloud properties and CCN by different Community Atmosphere Model (CAM) and Weather Research and Forecasting (WRF) Models are recommended for deep insight into the various mechanisms of ACPI over IGP.

Data Availability: The MODIS and TRMM data can be obtained from the NASA Goddard Earth Sciences Data and Information Center (GES DISC) and can be retrieved from the websites: https://modis.gsfc.nasa.gov/data/ and https://gpm.nasa.gov/data . The reanalysis-II datasets are obtained from the website: https://psl.noaa.gov/data/gridded/data.ncep.reanalysis2.html . The processed data used in this work are available on reasonable request from the corresponding author.

Author contribution: NG processed and analyzed the data and wrote the original draft of the manuscript. KA proposed the Idea, supervised this work, and revised the manuscript. YL helped in revising the manuscript.

Acknowledgment: The authors gratefully acknowledge the NASA Goddard Earth Sciences Data and Information Services Center (GES DISC) for the provision of freely available data retrieved from MODIS and TRMM. We are also grateful to the NOAA Physical Sciences Laboratory (PSL) for free accessibility to (NCEP/NCAR) reanalysis-II datasets.

References

Ackerman, A. S., Kirkpatrick, M. P., Stevens, D. E., & Toon, O. B.: The impact of humidity above stratiform clouds on indirect aerosol climate forcing, *Nature., 432*, 1014-1017, https://doi.org/10.1038/nature03174 , 2004.

Alam, K., Iqbal, M. J., Blaschke, T., Qureshi, S., & Khan, G.: Monitoring spatio-temporal variations in aerosols and aerosol–cloud interactions over Pakistan using MODIS data, Adva. Space Res., *46*, 1162-1176, https://doi.org/10.1016/j.asr.2010.06.025, 2010.

Alam, K., Qureshi, S., & Blaschke, T.: Monitoring spatio-temporal aerosol patterns over Pakistan based on MODIS, TOMS and MISR satellite data and a HYSPLIT model, Atmos. Envi., *45*, 4641-4651, https://doi.org/10.1016/j.atmosenv.2011.05.055, 2011.

Albrecht, B. A.: Aerosols, cloud microphysics, and fractional cloudiness, Sci., *245*, 1227-1230, https://doi.org/10.1126/science.245.4923.122 , 1989.

Ali, G., Bao, Y., Ullah, W., Ullah, S., Guan, Q., Liu, X., . . . Ma, J.: Spatiotemporal trends of aerosols over urban regions in Pakistan and their possible links to meteorological parameters, Atmo., 11, 306, https://doi.org/10.3390/atmos11030306, 2020.

Andreae, M., & Rosenfeld, D.: Aerosol–cloud–precipitation interactions. Part 1. The nature and sources of cloud-active aerosols, Earth. Sci. Rev., *89*, 13-41, https://doi.org/10.1016/j.earscirev.2008.03.001, 2008.

Anttila, T., Brus, D., Jaatinen, A., Hyvärinen, A. P., Kivekäs, N., Romakkaniemi, S., ... & Lihavainen, H.: Relationships between particles, cloud condensation nuclei and cloud droplet activation during the third Pallas Cloud Experiment, *Atmos. Chem. Phy.*, *12*, 11435-11450, https://doi.org/10.5194/acp-12-11435-2012 , 2012.

Anwar, K., Alam, K., Liu, Y., Huang, Z., Huang, J., & Liu, Y.: Analysis of aerosol cloud interactions with a consistent signal of meteorology and other influencing parameters, Atmos. Res., *275*, 106241, https://doi.org/10.1016/j.atmosres.2022.106241, 2022.

Brenguier, J.-L., Pawlowska, H., Schüller, L., Preusker, R., Fischer, J., & Fouquart, Y.: Radiative properties of boundary layer clouds: Droplet effective radius versus number concentration, Atmos. Sci., *57*, 803-821,https://doi.org/10.1175/1520-0469(2000)057<0803:RPOBLC>2.0.CO;2 , 2000.

Chen, F., Sheng, S., Bao, Z., Wen, H., Hua, L., Paul, N. J., & Fu, Y. : Precipitation Clouds Delineation Scheme in Tropical Cyclones and Its Validation Using Precipitation and Cloud Parameter Datasets from TRMM, Applied Met. Climatology. 57, 821-836,https://doi.org/10.1175/JAMC-D-17-0157.1 , 2018.

Chen, Q., Yin, Y., Jin, L.-j., Xiao, H., & Zhu, S.: The effect of aerosol layers on convective cloud microphysics and precipitation, Atmos. Res., *101*, 327-340, https://doi.org/10.1016/j.atmosres.2011.03.007, 2011

Costantino, L., & Bréon, F.: Analysis of aerosol-cloud interaction from multi-sensor satellite observations, Atmos. Sci., *37*,https://doi.org/10.1029/2009GL041828, 2010

Fan, C., Ding, M., Wu, P., & Fan, Y.: The Relationship between Precipitation and Aerosol: Evidence from Satellite Observation, Atmos. Oce. Phy.,https://doi.org/10.48550/arXiv.1812.02036, 2018.

Feingold, G., Eberhard, W. L., Veron, D. E., & Previdi, M.: First measurements of the Twomey indirect effect using ground-based remote sensors, Geophy. Res. Let., *30*, https://doi.org/10.1029/2002GL016633, 2003.

Gryspeerdt, E., Quaas, J., & Bellouin, N.: Constraining the aerosol influence on cloud fraction, *JGR.Atmos*,*121*, 3566-3583,https://doi.org/10.1002/2015JD023744 , 2016.

Guo, J., Su, T., Chen, D., Wang, J., Li, Z., Lv, Y., Zhai, P.: Declining summertime local-scale precipitation frequency over China and the United States, 1981–2012: The disparate roles of aerosols. *Geophy.Res.Letrs.*, *46*(22), 13281-13289, https://doi.org/10.1029/2019GL085442 ,2019.

Hassan, M. A., Mehmood, T., Liu, J., Luo, X., Li, X., Tanveer, M., & Abid, M.: A review of particulate pollution over Himalaya region: Characteristics and salient factors contributing ambient PM pollution. Atmos. Envi., 294, 119472, https://doi.org/10.1016/j.atmosenv.2022.119472 , 2002.

Hong, Y., Hsu, K. L., Moradkhani, H., & Sorooshian, S.: Uncertainty quantification of satellite precipitation estimation and Monte Carlo assessment of the error propagation into hydrologic response, Wat. Resc. Res., 42, 8, https://doi.org/10.1029/2005WR004398 , 2006.

Hossain, F., Anagnostou, E. N., & Bagtzoglou, A.: On Latin Hypercube sampling for efficient uncertainty estimation of satellite rainfall observations in flood prediction, Comp. & geosc., 32, 6, 776-792, https://doi.org/10.1016/j.cageo.2005.10.006 , 2006.

Houze Jr, R. A. Nimbostratus and the separation of convective and stratiform precipitation. In International geophysics. Elsevier. 104, 141-163, 2014.

Jiang, H., Feingold, G., & Cotton, W.: Simulations of aerosol-cloud-dynamical feedbacks resulting from entrainment of aerosol into the marine boundary layer during the Atlantic Stratocumulus Transition Experiment, JGR. Atmos., *107*, AAC 20-1-AAC 20-11, https://doi.org/10.1029/2001JD001502, 2002.

Jung, E.: Aerosol-cloud-precipitation interactions in the trade wind boundary layer, Ph.D Thesis, Meteorology and Physical Oceanography, University of Miami, 91-pp., 2012.

Kang, N., Kumar, K. R., Yin, Y., Diao, Y., Yu, X.: Correlation analysis between AOD and cloud parameters to study their relationship over China using MODIS data (2003-2013): impact on cloud formation and climate change,AAQR.,*15*, 958-973,https://doi.org/10.4209/aaqr.2014.08.0168 , 2015.

Kaskaoutis, D., Kumar Kharol, S., Sinha, P., Singh, R., Kambezidis, H., Rani Sharma, A.: Extremely large anthropogenic-aerosol contribution to total aerosol load over the Bay of Bengal during winter season, Atmos. Chem. Phy., *11*, 7097-7117, https://doi.org/10.5194/acp-11-7097-2011 , 2011.

Kedia, S., Ramachandran, S., Holben, B., & Tripathi, S.: Quantification of aerosol type, and sources of aerosols over the Indo-Gangetic Plain,Atmos.Envi.,, *98*, 607-619,https://doi.org/10.1016/j.atmosenv.2014.09.022, 2014.

Koike, M., Asano, N., Nakamura, H., Sakai, S., Nagao, T., & Nakajima, T.: Modulations of aerosol impacts on cloud microphysics induced by the warm Kuroshio Current under the East Asian winter monsoon, JGR. Atmos.,*121*,282-297,https://doi.org/10.1002/2016JD025375, 2016.

Koren, I., Kaufman, Y. J., Remer, L. A., & Martins, J. V.: Measurement of the effect of Amazon smoke on inhibition of cloud formation. Sci., 303(5662), 1342-1345, https://doi.org/10.1126/science.1089424, 2004.

Kubar, T., Hartmann, D., & Wood, R.: Understanding the importance of microphysics and macrophysics for warm rain in marine low clouds. Part I: Satellite observations, Atmos. Sci. 66, 2953-2972, https://doi.org/10.1175/2009jas3071.1, 2009.

Kumar, A., & Physics, S.: Variability of aerosol optical depth and cloud parameters over North Eastern regions of India retrieved from MODIS satellite data,Atmos. Sol. Terr. Phy.,*100*, 34-49,https://doi.org/10.1016/j.jastp.2013.03.025, 2013.

Kump, L. R., & Pollard, D.: Amplification of Cretaceous Warmth by Biological Cloud Feedbacks, Sci., *320*, 195-195,https://doi.org/10.1126/science.1153883, 2008.

Li, J., Lv, Q., Zhang, M., Wang, T., Kawamoto, K., Chen, S., & Zhang, B.: Effects of atmospheric dynamics and aerosols on the fraction of supercooled water clouds, *Atmos. Chem. Phy.*, *17*, 1847-1863,https://doi.org/10.5194/acp-17-1847-2017, 2017.

López-Romero, J., Montávez, J., Jerez, S., Lorente-Plazas, R., Palacios-Peña, L., & Jiménez-Guerrero, P.: Precipitation response to aerosol–radiation and aerosol–cloud interactions in regional climate simulations over Europe. *Atmos. Chem. Phys., 21*, 415-430, https://doi.org/10.5194/acp-21-415-2021 , 2021.

Masmoudi, M., Chaabane, M., Tanré, D., Gouloup, P., Blarel, L., & Elleuch, F.: Spatial and temporal variability of aerosol: size distribution and optical properties, Atmos. Res., *66*, 1-19,https://doi.org/10.1016/S0169-8095(02)00174-6 , 2003.

McCoy, D., Field, P., Schmidt, A., Grosvenor, D., Bender, F., Shipway, B.,& Elsaesser, G.: Aerosol midlatitude cyclone indirect effects in observations and high-resolution simulations, *Atmos. Chem. Phy.*, *18*, 5821-5846, https://doi.org/10.5194/acp-18-5821-2018 , 2018.

Michibata, T., Kawamoto, K., & Takemura, T.: The effects of aerosols on water cloud microphysics and macrophysics based on satellite observations over East Asia and the North Pacific, Atmos. Chem. Phy., *14*, 10515-10541, https://doi.org/10.5194/acp-14-11935-2014 , 2014.

Myhre, G., Stordal, F., Johnsrud, M., Kaufman, Y., Rosenfeld, D., Storelvmo, T.: Aerosol-cloud interaction inferred from MODIS satellite data and global aerosol models, Atmos. Chem. Phy., *7*, 3081-3101, https://doi.org/10.5194/acp-7-3081-2007, 2007.

Nair, V., Giorgi, F., Keshav Hasyagar, U.: Amplification of South Asian haze by water vapour–aerosol interactions, Atmos,Chem.Phy., *20*, 14457-14471, https://doi.org/10.5194/acp-20-14457-2020 ,2020.

Naud, C., Posselt, D., & van den Heever, S.: Observed covariations of aerosol optical depth and cloud cover in extratropical cyclones, *JGR: Atmos*,*122*,10-338,https://doi.org/10.1002/2017JD027240 , 2017.

Rossow, W., & Schiffer, R.: Advances in understanding clouds from ISCCP, Bul. Americ. Meteor. Soci., *80*, 2261-2288, https://doi.org/10.1175/15200477(1999)080<2261:AIUCFI>2.0.CO;2 ,1999.

Sharma, P., Ganguly, D., Sharma, A., Kant, S., Mishra, S.: Assessing the aerosols, clouds and their relationship over the northern Bay of Bengal using a global climate model, Earth. Spac. Sci., *10*, e2022EA002706, https://doi.org/10.1029/2022EA002706, 2023.

Sherwood, S., Roca, R., Weckwerth, T., & Andronova, N.: Tropospheric water vapor, convection, and climate, Rev. of Geophy (AGU), 48, 2,https://doi.org/10.1029/2009RG000301, 2010.

Singh, A., Rastogi, N., Sharma, D., Singh, D.: Inter and intra-annual variability in aerosol characteristics over northwestern Indo-Gangetic Plain,AAQR., *15*, 376-386,https://doi.org/10.4209/aaqr.2014.04.0080, 2015.

Srivastava, P., Pal, D., Aruche, K., Wani, S., & Sahrawat, K.: Soils of the Indo-Gangetic Plains: a pedogenic response to landscape stability, climatic variability and anthropogenic activity during the Holocene, Earth. Sci. Rew., *140*, 54-71, https://doi.org/10.1016/j.earscirev.2014.10.010, 2015.

Stevens, B., & Feingold, G.: Untangling aerosol effects on clouds and precipitation in a buffered system, Nature, 461, 607-613,https://doi.org/10.1038/nature08281 , 2009.

Sun, J., & Ariya, P.: Atmospheric organic and bio-aerosols as cloud condensation nuclei (CCN): A review, Atmos. Envi., 40, 795-820,https://doi.org/10.1016/j.atmosenv.2005.05.052 , 2006.

Tao, W., Chen, J., Li, Z., Wang, C., & Zhang, C.: Impact of aerosols on convective clouds and precipitation, Rev. Geophys., *50*,https://doi.org/10.1029/2011RG000369, 2012.

Thomas, A., Kanawade, V., Sarangi, C., & Srivastava, A.: Effect of COVID-19 shutdown on aerosol direct radiative forcing over the Indo-Gangetic Plain outflow region of the Bay of Bengal,Sci. Total Envi., *782*, 146918,https://doi.org/10.1016/j.scitotenv.2021.146918, 2021.

Tian, Y., & Peters-Lidard, C.: A global map of uncertainties in satellite-based precipitation measurements, Geohys. Res. Let., 37, 24, https://doi.org/10.1029/2010GL046008 , 2010.

Tripathi, S. N., Pattnaik, A., & Dey, S.: Aerosol indirect effect over Indo-Gangetic plain, Atmos. Envi., 41, 33, 7037-7047, https://doi.org/10.1016/j.atmosenv.2007.05.007, 2007.

Twomey, S.: The influence of pollution on the shortwave albedo of clouds, Atmos. Sci., *34*, 1149-1152,https://doi.org/10.1175/1520-0469(1977)034<1149:TIOPOT>2.0.CO;2 , 1977.

Verma, S., Ramana, M., & Kumar, R.: Atmospheric rivers fueling the intensification of fog and haze over Indo-Gangetic Plains, Sci. Reports., Nature, *12*, 5139, 2022.

Wang, F., Guo, J., Zhang, J., Huang, J., Min, M., Chen, T., Li, X.: Multi-sensor quantification of aerosol-induced variability in warm clouds over eastern China. *Atmos. Envi.*, *113*, 1-9, https://doi.org/10.1016/j.atmosenv.2015.04.063 , 2015.

Wolf, E., & Toon, O.: Controls on the Archean climate system investigated with a global climate model, Astrobiology, *14*, 241-253,https://doi.org/10.1089/ast.2013.1112, 2014.

Wood, R.: Relationships between optical depth, liquid water path, droplet concentration, and effective radius in adiabatic layer cloud,University of Washington, *3*, 2006.

Wu, P., Dong, X., Xi, B., Liu, Y., Thieman, M., & Minnis, P.: Effects of environment forcing on marine boundary layer cloud-drizzle processes, JGR: Atmos., *122*, 4463-4478,https://doi.org/10.1002/2016JD026326, 2017.

Wyant, M., Bretherton, C., Bacmeister, J., Kiehl, J., Held, I., Zhao, M., Soden, B.: A comparison of low-latitude cloud properties and their response to climate change in three AGCMs sorted into regimes using mid-tropospheric vertical velocity, Clim. Dyn., *27*, 261-279, https://doi.org/10.1007/s00382-006-0138-4, 2006.

Yuan, T.: Increaseofclouddropletsizewith aerosolopticaldepth: Anobservationandmodelingstudy, JGR: Atmos., *113*, D4, https://doi.org/10.1029/2007JD008632, 2008.

Yang, Y., Liu, X, Qu, Y., An, J., Jiang, R., Zhang, Y., & Ma, Q. : Characteristics and formation mechanism of continuous hazes in China: a case study during the autumn of 2014 in the North China Plain. ACP., 15, 8165-8178, https://doi.org/10.5194/acp-15-8165-2015, *2015*.

Zeb, B., Alam, K., Sorooshian, A., Chishtie, F., Ahmad, I., Bibi, H.: Temporal characteristics of aerosol optical properties over the glacier region of northern Pakistan, Jour. Atmos. Sol-Terr. Phy., *186*, 35-46,https://doi.org/10.1016/j.jastp.2019.02.004, 2019.

Zhao, C., Tie, X., & Lin, Y.: A possible positive feedback of reduction of precipitation and increase in aerosols over eastern central China, Geo. Res. Let., 33, 11, https://doi.org/10.1029/2006GL025959, 2006.

Zhou, S., Yang, J., Wang, W., Zhao, C., Gong, D., Shi, P.: An observational study of the effects of aerosols on diurnal variation of heavy rainfall and associated clouds over Beijing–Tianjin–Hebei, Atmos. Chem. Phy., *20*, 5211-5229,https://doi.org/10.5194/acp-20-5211-2020, 2020.